The relation between dye-filling and ivermectin resistance in *Caenorhabditis elegans*

Vittoria Lipari
Department of Biology, McGill University, Montreal
July 2018

A thesis submitted to McGill University in partial fulfillment of the requirements of the degree
Master of Science

Contents

1. Abstract

Parasites are a global issue across the globe. In the Canadian livestock industry, resistance to commonly used drugs leads to significant losses in productivity and profit. The study of anthelminthics such as ivermectin is thus beneficial to finding new ways to protect mammals from these parasites and to increase farming income. We are interested in genes that confer both ivermectin resistance and a dye-filling defective phenotype, called *dyf* genes, when mutated. *Dyf* genes are of interest because they have been shown to be associated with ivermectin resistance in the model nematode *Caenorhabditis elegans* and in parasites such as *Haemunchus contortus*, however the mechanisms of resistance remain unclear. In this project, we investigate three mechanisms by which the *dyf* genes might confer ivermectin resistance: either by altering drug entry, communication within the nervous system, and/or stress response pathways. Our results suggest that drug entry plays an important role in ivermectin resistance, although it is unclear whether importance lies in dye-filling neurons or neurons with direct connections to glutamate-gated chloride channels. Additionally, the subset of P-glycoprotein efflux pump genes *pgp-1*, *pgp-2*, *pgp-3*, *pgp-9*, and *mrp-1* is essential in maintaining ivermectin resistance in the *dyf-7* mutant.

La résistance des parasites aux médicaments dans l'industrie d'élevage est un problème important pour les fermiers puisque cela cause d'énormes déficits en profit et en productivité chaque année. Par conséquent, il est important d'étudier les antihelminthes comme l'ivermectine pour mieux comprendre la méthode de résistance et de trouver des solutions pour protéger l'industrie d'élevage. On est intéressé à un groupe de gènes qui cause la résistance à l'ivermectine et qui empêche l'absorption de colorant, dont les gènes *dyf*. On examine *dyf-7* parce que qu'elle a déjà été montré de conférer la résistance à l'ivermectine hors de l'environment des laboratoires, et par conséquent *dyf-3* parce qu'elle confère un niveau de résistance similaire à *dyf-7* et elle peut être exprimer dans les neurones sensoriels individuellement. Dans ce projet, on enquête le mécanisme dont les gènes *dyf* confère la résistance à l'ivermectine soit par : modifiant la manière que la drogue entre l'animal, éliminant ou modifiant la communication entre des différents neurones, ou en éliminant ou modifiant des réponses au stress. Nos résultats suggèrent que l'entrent d'ivermectine par les neurones sensoriels est impératif pour conférer la résistance à la drogue. De plus, la mutation collective des gènes de pompe d'efflux de p-glycoprotéines *pgp-1*, *pgp-2*, *pgp-3*, *pgp-9*, et *mrp-1* est essentielle pour maintenir la résistance dans les animaux avec la mutation en *dyf-7*.

2. Acknowledgements

I would like to thank Joseph Dent, Ph.D. for his endless support and mentorship in this project, and Robin Beech, Ph.D., both of which supported this project as co-supervisors. I would also like to thank Michael Hendricks, Ph.D. for being part of the supervisory committee and for offering me the resources to complete certain experiments. Additionally, I would like to thank Chris Farnet, Ph.D. for providing strains and other materials used in this project, as well as his patience for my numerous questions. Finally, I would like to acknowledge Gayatri Suresh, James Bae, and Katia Fox for providing some of the strains and data used in this project. James provided Figure 5, based on his own research. Katia performed ivermectin dose response assays on various mutants involved in transferring signals between neurons including innexins (Inx-7, Inx-18, Inx-19, Che-7, and Unc-9), a glutamate transporter (Eat-4), and a neuropeptide transporter (Unc-31). Gayatri provided the *pgp-1(pk17)::pgp-2(gk114)::pgp-3(pk18)::pgp-9(tm830)::mrp-1(pk89)::dyf-7(m153)* strain.

3. Preface

Since September 2016 I have worked on my master's research project, on the topic of ivermectin resistance in free-living and parasitic nematodes alike. In this thesis, I explain why drug resistance is so important and how this promising line of research may lead us to solve a growing issue. This dissertation was written to fulfill the graduation requirements for the McGill University Master of Science Biology program. I would like to note that Gayatri Suresh contributed to this project by creating a strain (JD712) and Katia Fox collected data for the dose response curves of the following strains: MT6308, RB1896, RB1792, DA509, RB1834, CX6161, CF1038, PS3551, and RB1373.

4. Introduction

Parasitic nematodes are responsible for lost productivity in the livestock industry worldwide. A common solution to this issue is administering anthelmintics such as macrolytic lactones on a regular, preventative basis, however this has encouraged nematodes to develop resistance to these drugs. Drug resistance is a global issue affecting all the major agricultural producers. In New Zealand, approximately 25% of parasite-infected sheep herds and 92% of infected cattle herds harbor parasites that are resistant to the macrolytic lactone ivermectin [1, 2]. Closer to home, as many as 76% of U.S. farms infected with the sheep parasite *Heamonchus contorus* are resistant to ivermectin [3]. The lack of data from Canadian flocks makes it difficult to stage macrolytic lactone resistance, however preliminary studies suggest that as much as 89% of Ontario sheep flocks have nematode parasite infections and in 97% of these flocks, the parasites are resistant to ivermectin [4].

The importance of maintaining the efficacy of anthelmintics is reflected in the value they add to livestock. Effective anthelminthic treatment can increase Angus calf weight by an average of 15.5kg. [5] An increase in 15kg in Quebec is equivalent to an additional $42.71 per head on average, which could have increased sales by $17.3 million in Quebec alone if parasite resistance prevalence is similar to that of Ontario (based on AIMIS January 2018 values). Similarly, effective anthelmintic treatment on sheep herds can increase body weight by 4.7kg on average [6]. This translates to a $877.5k increase in profits when sold in Quebec (based on AIMIS January 2018 values). Additionally, such treatments allow sheep to reach their target weight sooner than untreated or unsuccessfully treated herds, thereby decreasing the cost of feeding and maintenance per head, thus further increasing productivity [6]. With such potential to increase efficiency in the livestock industry, it is important to understand resistance mechanisms and search for effective parasite treatments.

The purpose of this project is to investigate the mechanism of ivermectin resistance conferred through the mutation of the dye-filling (*dyf*) genes. In the sheep parasite *H. contortus*, *dyf-7* mutations appear in animals selected for ivermectin resistance and confer sensory neuron defects [7]. In this project, we use *C. elegans* as a non-parasitic model nematode because of its

simplicity and ease of use in the lab. The goal is to apply results drawn from *C. elegans* to parasitic nematodes such as *H. contortus*. We believe *C. elegans* is a relevant model because it shares several orthologous genes with its parasite counterparts, including *dyf-7,* that are related to both ivermectin sensitivity and resistance *[7]*.

We examine two hypotheses to explain the ivermectin resistance of *dyf* genes: 1) that the resistance mechanism works by altering drug entry through the sensory neurons, and 2) the absence of sensory input in *dyf* mutants activates systemic stress response mechanisms that alter drug sensitivity. We will test these hypotheses in three sets of experiments. First, we predict that if sensory neurons are a site of drug entry, then the sensitivity of the worms to ivermectin will correlate with the number of sensory neurons that are defective. Whereas if the drug resistance is the result of sensory neurons no longer responding to external sensory cues, which in turn alters gene expression and drug metabolism, then we expect ivermectin resistance to correlate with the function of neurons that have specific sensory modalities.

In the second part of this project, we ask whether neuronal signal propagation by sensory neurons is necessary for ivermectin resistance pathway. If the defective sensory neurons in the *dyf* mutant are activating a stress response, then they must activate the stress response via some form of neurotransmission. If so, mutants that are defective in neurotransmission should exhibit altered sensitivity to ivermectin. Alternatively, if sensory neurons are passive portals of drug entry, then neural communication should not be necessary for ivermectin resistance, we expect to see no change in sensitivity in neurotransmission mutants.

Finally, we wish to know whether certain stress responses themselves are necessary for ivermectin resistance in *C. elegans*. If the *dyf* resistance pathway is dependent on the function or upregulation of a stress response pathway, then we predict that mutants with altered stress responses will affect ivermectin resistance. Otherwise, if sensory neurons are ports of drug entry, then we will see no change in resistance when the stress response pathways are activated or reduced.

5. Background

5.1. Effects of avermectins on parasitic nematodes

Ivermectin belongs to the chemical family of avermectins, which are naturally produced by the soil fermenter *Steptomyces avermitilis* during the bacteria's fermentation process. These 16-membered compounds (shown in figure 1) activate glutamate-gated chloride channels (GlucCls) found on the muscle and nerve cells of nematodes, insects, arachnids, and arthropods [8].

Figure 1. Chemical structures of avermectin $B_{1\alpha}$ (left), ivermectin $B_{1\alpha}$ (center), and milbemycin A_4 (right). [8]

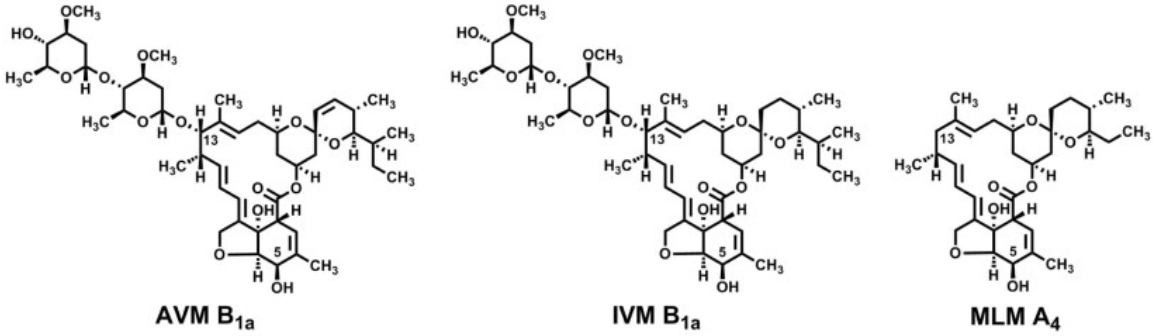

The GluCls are transmembrane channels for chloride ions in nerve and muscle cells. Gating of the channels by neurotransmitters is a necessary step in neuron signal propagation at inhibitory glutamatergic synapses[8]. Ivermectin binds allosterically and irreversibly activates the GluCls, allowing free flow of chloride into the neuron and thus preventing further action potentials, resulting in locomotor and pharyngeal paralysis [9]. How ivermectin reaches its target is currently unknown and is the focus of this project.

5.2. Genes related to ivermectin resistance and C. elegans amphid structure

The body of *C. elegans* is nearly impenetrable by drugs except where their sensory neurons are exposed to the environment through a structure known as the amphid channel (shown in figure 2). The nematode head has two amphid channels where the cilia from each pair of 8 sensory neuron dendrites are exposed to the environment [10]. The sensory dendrites in the amphid channels originate from neuronal soma in the head, which in turn have axons that extend into the nerve ring

(brain) of the animal. A few other sensory neurons are found at the head of *C. elegans* not at the amphid channel. Of these neurons, the IL2 cilia are also exposed to the external environment and are found in the inner labial sensilla (see figure 2) [10].

Figure 2. Shows structure of the amphid with some of the sensory neurons (left). The socket cell (so) surrounds and forms the amphid channel, which is further lined with cuticle. The sheath cell (sh) borders the amphid channel where 4 sensory neurons penetrate it (AWA, AWB, AWC, and AFD). The inner labial sensilla (right) contains other sensory neurons, of which IL1 is embedded in cuticle and IL2 is exposed to the external environment. [10]

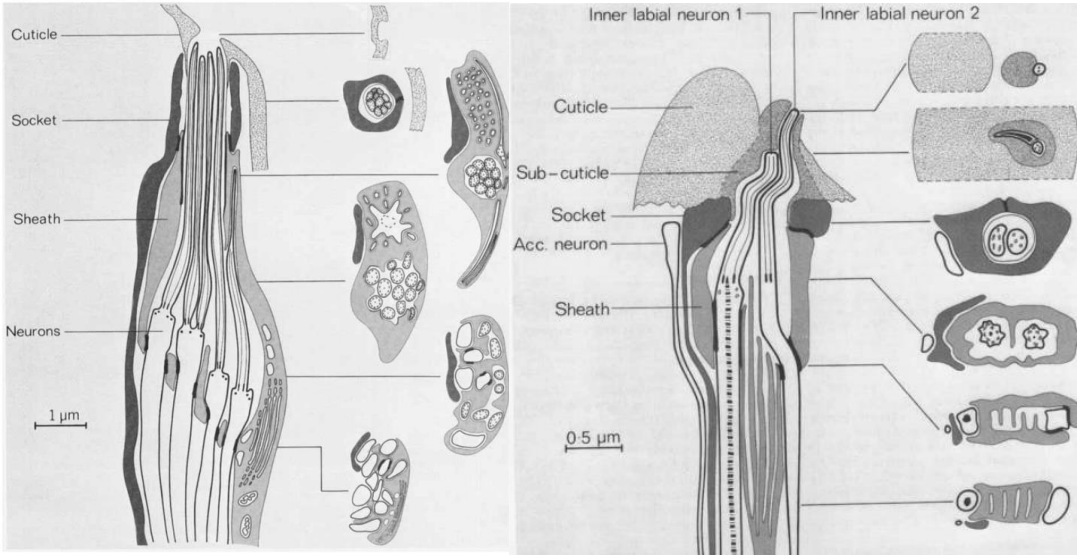

The sensory neurons have specialised functions. Figure 3 shows a table listing the sensory neurons and their general roles. ASE senses and causes the nematode to move towards certain chemicals, particularly Na+ (left neuron), Cl- (right neuron), cAMP, biotine, lysine, and serotonin [11, 12]. The ADF, ASG, ASI, and ASK neurons also play minor roles in chemoattraction. Removal of ADF, ASG, ASI, or ASJ prior to the first larval molt forces the nematode into the dauer stage, which is a growth-arrested, stress-resistant form [13]. These same neurons are also involved in propagating signals that affect life span, where removal of ASI, ASG, and ADF signaling increases longevity, and loss-of-function of ASJ and ASK decreases life span only when ASI is ablated [14]. These neurons are thought to affect life span through the Daf-2 Insulin/IGF-1 signaling pathway [14]. In another stress response pathway, ASH and ASI stimulation results in downregulation of the unfolded protein response, a stress response necessary for innate immunity [15]. When ASH senses high osmolarity, heavy metals, detergents, acid pH, and some organic

compounds, it will also cause a change in direction of *C. elegans* away from the stimulant. The ADL neuron is also involved in chemorepulsion [11]. IL2 is presumably involved in chemosensory stimulation.

Figure 3. List of the sensory neurons in and around the amphid and labial sensilla of C. elegans along with their exposure, dye-filling status, and their general role. Neurons labelled in red are known to absorb dye. (Adapted from Inglis 2006 [16]).

Ciliated neuron	Exposed to the environment?	Embedded in	Dye-fills?	General Role
ASE	Yes	-	No	Chemoattraction
ADF	Yes	-	Yes	Dauer entry
ASG	Yes	-	No	Dauer entry, Chemoattraction
ASH	Yes	-	Yes	Mechanosensory, chemorepulsion, osmo-avoidance
ASI	Yes	-	Yes	Dauer entry, Chemoattraction
ASJ	Yes	-	Yes	Dauer exit/recovery
ASK	Yes	-	Yes	Chemoattraction
ADL	Yes	-	Yes	Chemorepulsion
AWA	No	Sheath cell	No	Chemoattraction
AWB	No	Sheath cell	No	Chemorepulsion
AWC	No	Sheath cell	No	Chemoattraction
AFD	No	Sheath cell	No	Thermosensation
ADE	No	Subcuticle	No	Mechanosensation
IL1	No	Subcuticle	No	Mechanosensation
IL2	Yes	-	Occasionally	Chemosensory
OLQ	No	Subcuticle	No	Mechanosensation
OLL	No	Subcuticle	No	Mechanosensation
CEP	No	Subcuticle	No	Mechanosensation
CEM	Yes	-	No	Mechanosensation
BAG	No	Behind cuticle	No	
FLP	No	Behind cuticle	No	Mechanosensation

5.3. Dye-filling in nematodes

The importance of the amphids in allowing chemosensory neurons access to the environment is evident from the ability of amphid neurons to be dye-filled. Nematodes can absorb dye from the environment via certain exposed sensory neurons, shown in red in figure 3. The molecular structure of the dyes used in this project are shown in Figure 4. DiO is a stain that causes 6 sensory neurons to fluoresce green whereas DiI emits a red fluorescence from the neurons. Both of these molecules are bulky, lipophilic compounds, similar to ivermectin. Interestingly, ivermectin resistance has been linked to mutations that prevent the uptake of dye from the environment [17]. Most of the known dye-filling defective (dyf) mutations result in morphologically irregular cilia on the sensory neuron dendrites, such as *dyf-3*, which will be discussed later. The only known exception is *dyf-7*, which affects dendrite length and thus the cilia access to the external environment. Some of the other known mutations that confer both ivermectin resistance and an inability to absorb dye are shown in figure 5. We believe that the conferred ivermectin resistance from these *dyf* mutations derives from the ability for the sensory neurons to uptake bulky, lipophilic molecules such as dyes and ivermectin from the environment.

Figure 4. Shows the molecular structure of ivermectin (left) [8], and the molecular formulas for DiI and DiO (accessed from pubchem June 2018).

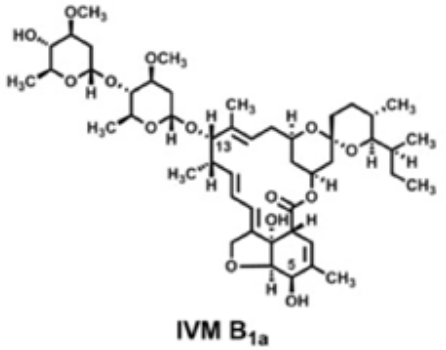

Compound	Molecular Formula
DiI	C59H97CIN2O4
DiO	C53H85CIN2O6

Figure 5. Shows various dye-filling defective mutations and their increasing resistance to ivermectin at 10ng/ml (blue bars). The red bars show the percent of non-dye-filling animals in each strain. James Bae, unpublished data.

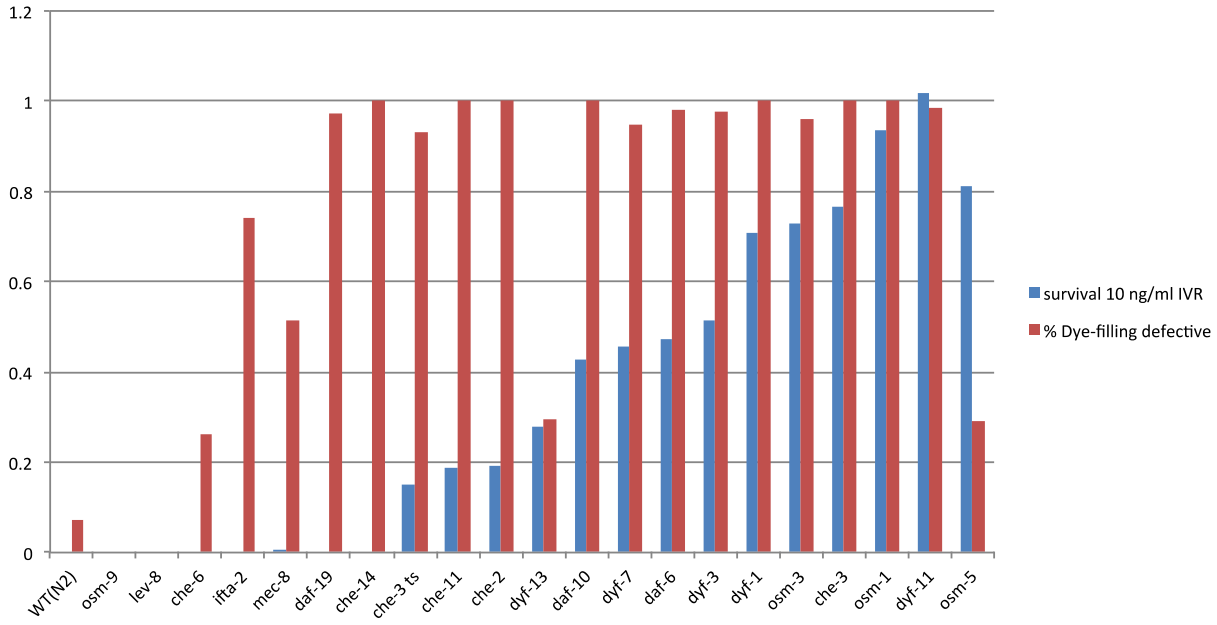

5.4. Role of *dyf-7* in ivermectin resistance

Mutations in all dyf genes alter the anatomy the sensory neurons of *C. elegans* such that they cannot take up fluorescent dyes from the environment. Most of these mutations affect the cilia at the end of the dendrites, however *dyf-7* is an exception where the mutation alters the length of the neuronal dendrites. In wild type embryonic *C. elegans*, the sensory neurons originate at the presumptive amphids and eventually elongate towards the nerve ring [18]. This mode of migration is called retrograde extension and is depicted in figure 6. *Dyf-7* animals develop similarly to the wild type, with the sensory neurons originating at the nose, however as the cell body migrates, the dendrites do not remain at the nose but instead migrate with the cell body towards the nerve ring. This is evidence that Dyf-7 is an anchoring protein [18].

During larva development, sensory neurons release Dyf-7 through their membrane, then proteases activate the protein so that it can attach to the amphid structure. Soon afterwards, neighbouring cells secrete another protein called Dex-1, which then works with Dyf-7 to anchor the dendrites [18]. Since Dyf-7 is a secreted protein, restoring gene function in one sensory neuron will result in anchoring and thus proper functioning of all sensory neurons. For the purposes of

this experiment, we wish to observe the role of specific neuron subsets in ivermectin resistance. For this reason, we choose to study *dyf-3* mutants in place of *dyf-7* mutants due to their similar ivermectin resistance level and because *dyf-3* is expressed cell autonomously.

Figure 6. Shows different modes of cell migration. The image on the far right shows retrograde extension with the cell body starting at the point of attachment and moving away from this point during development [18].

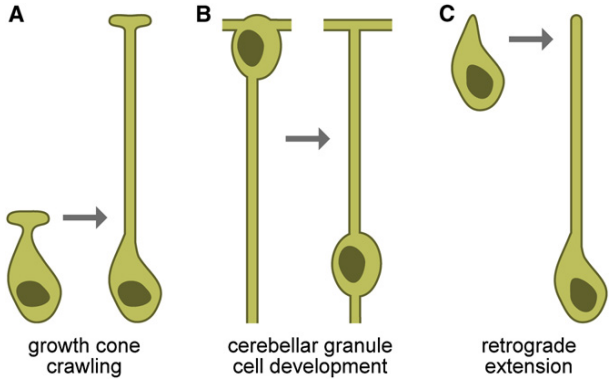

5.5. Sensory neuron cilia and relevance of *dyf-3*

Another *dyf* gene that confers similar resistance to ivermectin as the *dyf-7* mutant is *dyf-3*. *Dyf-3* encodes 3 proteins: Dyf-3A, Dyf-3B, and Dyf-3C [19]. These proteins form a subcomplex in the intraflagellar transport (IFT), which is the transport mechanism that the cells use to form cilia [19]. More specifically, the Dyf-3 proteins collectively form an IFT-B subcomplex (shown in Figure 7), which transports the building blocks of cilia and is thus necessary for proper cilia development [20]. A few of the known *dyf-3* mutations create a stop codon in the coding sequence so that the proteins are not synthesized and the IFT-B subcomplex cannot form properly [20]. This in turn creates shorter cilia that cannot take up dye from the environment. We are interested in *dyf-3* because it is expressed cell autonomously, unlike *dyf-7*, which is secreted and can restore sensory neuron dye-filling in all nearby cells [19]. Using *dyf-3* instead of *dyf-7* allows us to restore wild type dye-filling in the neurons that we choose. Eight of the sensory neurons have cilia exposed to the environment at the tip of their dendrites: ASE, ASG, ASH, ASI, ASJ, and ASK have a single cilium whereas ADF and ADL have two [10]. These exposed sensory neurons will be the target of the first set of experiments in this project.

Figure 7. Shows how non-motor sensory cilia are formed in nematodes and all the machinery required for proper cilia formation (left), and the effects of various protein mutations on ciliary formation (right). *Dyf-3* encodes proteins that form the IFT-B subcomplex and loss-of-function mutations lead to non-functional cilia. [20]

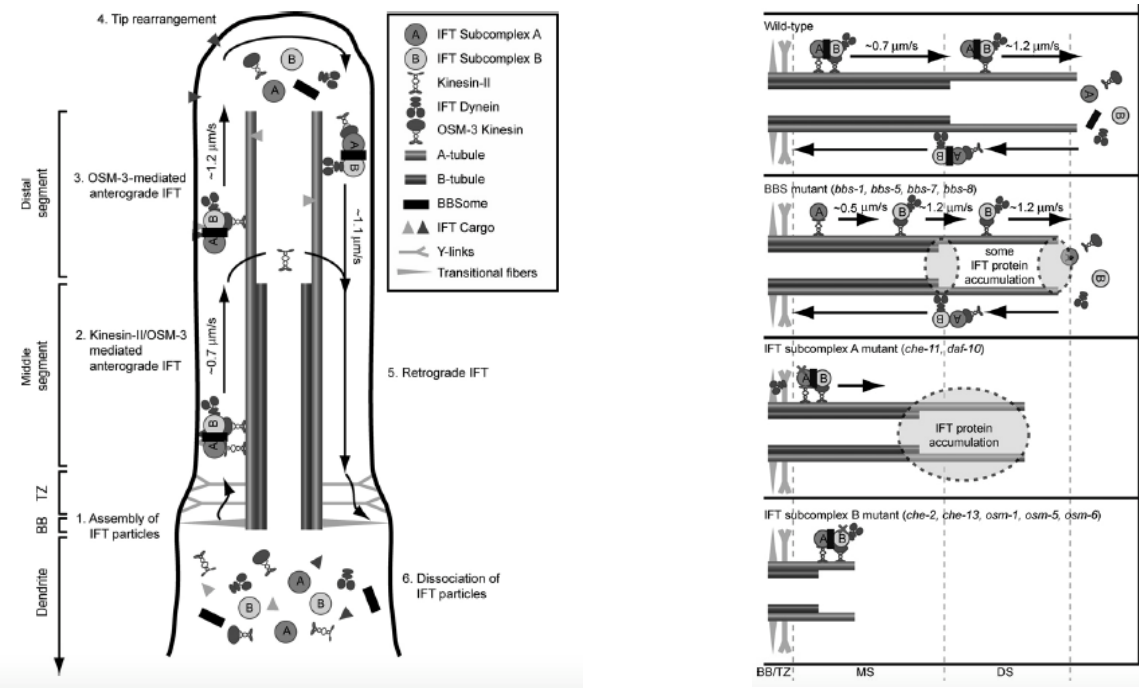

5.6. Ivermectin Pathway

The path ivermectin takes to reach its target, the GluCl's, is not yet understood. One possibility is that ivermectin enters the worm through the dye-filling sensory neurons in the amphid channel, then travels through the neurons to the interneurons in the nerve ring, then through these neurons to the GluCl expressed on the nerve and muscle cells, as depicted in figure 8. Once ivermectin has entered the animal, it is unclear how it diffuses throughout the body. Ivermectin is a lipophilic molecule that partitions strongly into lipid membranes but also has been shown capable of diffusing across lipid bilayers [21]. It is difficult to compare membrane permeability of ivermectin to water or ions across studies since the experimental conditions are very different, particularly cell pH and lipid length [21-23]. Whether ivermectin would be able to diffuse out of sensory neurons is unclear.

Alternatively, if *dyf* mutations do not confer ivermectin resistance by altering drug entry, then perhaps the lack of sensory input triggers metabolic changes, e.g. a stress response, that

renders the animal more resistant to ivermectin. We can determine this by testing whether or not ivermectin resistance in *dyf-7* worms is dependent on functional communication between the sensory neurons and the interneurons.

Figure 8. **The proposed pathway of ivermectin reaching the GluCl's.** First, ivermectin (IVM) enters the dendrites of the sensory neurons (red) and diffuses to the cell body (steps 1 and 2). From there, the ivermectin molecules diffuse through the interneurons (blue), motor neurons, and muscle cells (steps 3, 4, and 5). Finally, once in the synapse, ivermectin can bind to the GluCl on the post-synaptic cell and leave the channels open for chloride ions to pass freely through. The pathway shows the M3 motor neuron (green) and pm4 muscle as an example target for ivermectin, resulting in pharyngeal pumping paralysis.

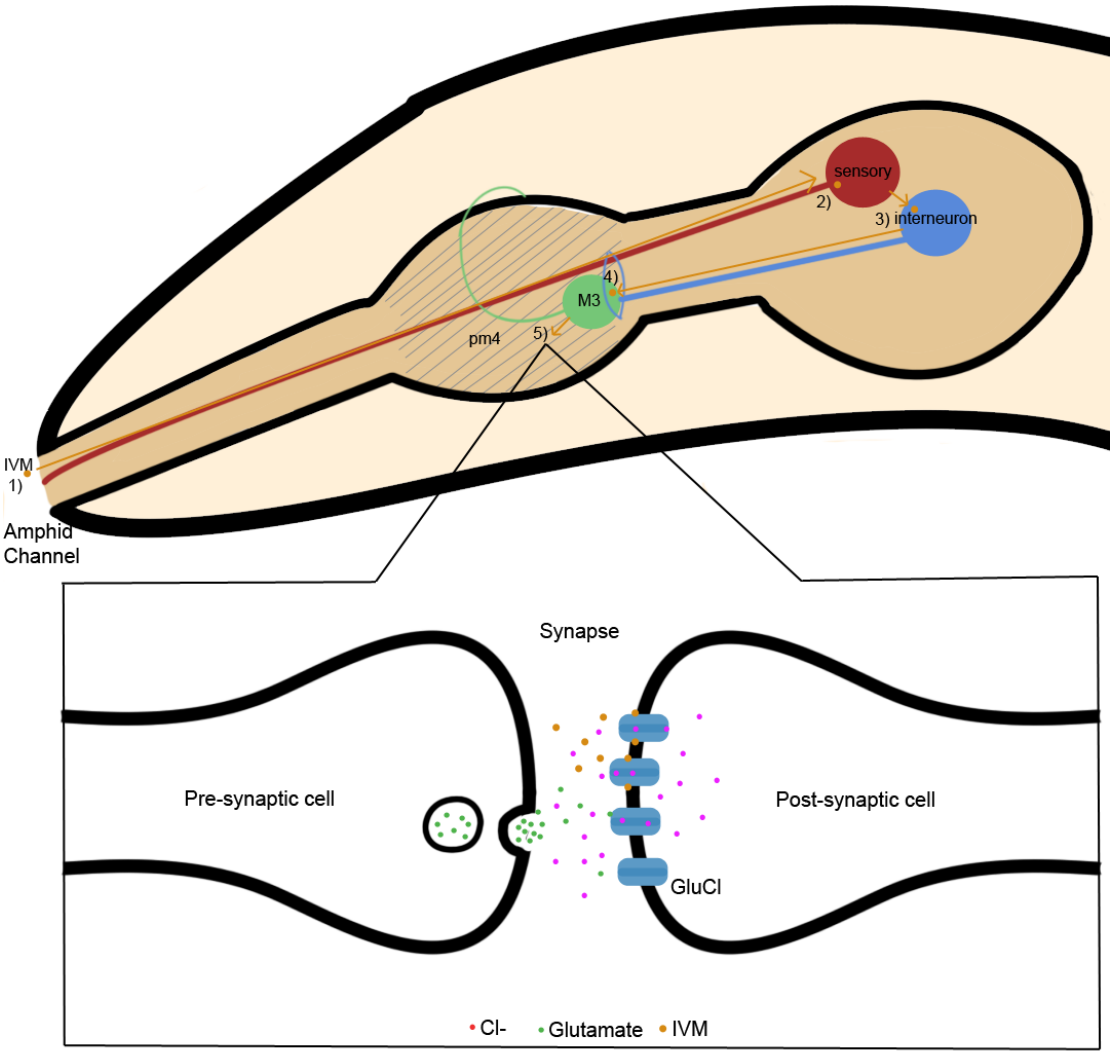

5.7. Genes involved in sensory neuron-to-interneuron communication

In *C. elegans*, there are several ways that the sensory neurons can communicate signals to the body muscles that may be necessary for the resistance mechanism. The first is via gap junctions between cells. The gap junctions are formed by six protein subunits of innexins and can be either homotypic (formed by two homomeric hemichannels on either adjoining membrane), heterotypic (formed by two different homomeric hemichannels on either membrane), or heteromeric (formed by heteromeric hemichannels on both membranes) [24]. The various channel types are shown in Figure 9. In total, there are 25 genes that code for innexins in *C. elegans*. The ones we are interested in are *inx-7, inx-18, che-7* (previously *inx-4*), and *unc-9* because they are all expressed in ASH and ASI and/or ADL sensory neurons, which are known to be involved to activate stress responses in *C. elegans*. ASI is necessary to trigger several stress responses, including the Daf-2 signaling pathway for longevity and dauer formation, and Daf-7/TGF-β mediated sex-specific behaviour [14, 25].

Figure 9. The various forms of gap junctions formed by innexins. Innexins can form either homomeric or heteromeric hemichannels or homotypic, hetertypic, or hetermeric intercellular channels. [26]

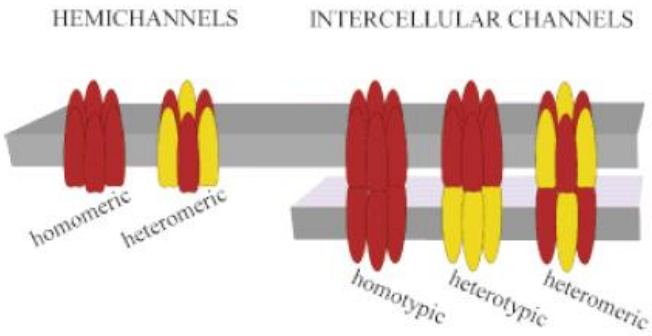

Inx-7 is one of the most widely expressed innexins in the *C. elegans* nervous system, being expressed in interneurons, sensory neurons, and the MC pharyngeal motor neuron [24]. The Unc-9 protein is another of the primary innexins found in the nervous system and its expression overlaps with that of Inx-7, suggesting that these proteins may form heteromeric channels. Additionally, Unc-9 is expressed in the M5, NSM, I1, I3, and I6 pharyngeal motor and interneurons. It also plays a role in ivermectin resistance, but only when coupled with mutations in the GluCl subunits [17]. Like Unc-9, Inx-18 is an innexin involved in signal propagation in muscle cells, specifically muscle electrical coupling [27]. Interestingly, recent research suggests that Inx-18 requires Unc-9 to form fully functional gap junctions for muscle electrical coupling but Unc-9 can potentially

form homotypic channels or heterotypic channels with another innexin in the body-wall muscles [27]. Finally, Che-7, previously known as Inx-4, is an innexin also found in the *C. elegans* nervous system and is specifically known to modulate quinine sensitivity in the ASH sensory neurons [28].

Another way the brain can communicate signals to the body is by releasing neurotransmitters and neuropeptides in vesicles. In general, neurotransmitters such as glutamate are packaged in small synaptic vesicles, while neuropeptides and biogenic amines are packaged in large dense-core vesicles. The synaptic vesicle packaging of glutamate is controlled by Eat-4 [29]. A mutation in *eat-4* leads to a defect in the packaging of glutamate into pre-synaptic vesicles, thereby weakening certain muscular responses such as pharyngeal pumping [30]. For larger neuropeptides, the CAPS protein Unc-31 is necessary for content release [31]. Unc-31 primes dense-core vesicles to respond to calcium concentration flux in the cell so that the neuropeptides can be released into the synapse [32].

5.8. Stress response in nematodes

Upregulated or wild-type stress response mechanisms may support *dyf* mutation resistance by altering the pharmacokinetics of ivermectin either by metabolizing ivermectin or removing it from cells. We can test this by manipulating various stress response pathways and determining if they are necessary for ivermectin resistance in the *dyf-7* mutants.

Nematodes handle various stress-inducing molecules in three phases. In phase I, the body cells solubilise lipophilic xenobiotics with enzymes such as cytochrome p450's. Phase II includes enzymes that detoxify harmful substances such as reactive oxygen species or those targeted by phase I. Finally, phase III enzymes remove xenobiotics from the system via transporters. The ABC transporters and multi-drug resistance protein (mrp) transporters fall into this category [33]. Skn-1, a transcription factor, has been shown to regulate genes in all three phases of stress responses [34, 35].

Skn-1 is homologous to the mammalian Nrf/CNC family of transcription factors. The genes share much of their DNA sequence, although unlike its homolog, Skn-1 can bind and transcribe

DNA without a basic leucine zipper [34]. Skn-1 is expressed in ASI and intestinal cells and increased expression results in increased resistance to oxidative stress and increased longevity. Skn-1 is regulated through the same signaling pathway as the FOXO transcription factor Daf-16, shown in figure 10. Both transcription factors are downregulated by insulin/IGF-1-like signaling (IIS), which is mediated through the Daf-2 receptor [36]. Daf-2 mutants accumulate Daf-16 and Skn-1 in nuclei and from dauer larva constitutively. Another transcription factor, Hsf-1 (heat-shock factor) is also controlled by IIS (reviewed in [37]). When the cells reduce IIS, Daf-16, Skn-1, and Hsf-1 are active and promote longevity, stress resistance, and bacterial resistance [37, 38].

Figure 10. Shows the IIS pathway and how it regulates the Daf-16 and Skn-1 transcription factors. [36, 39]

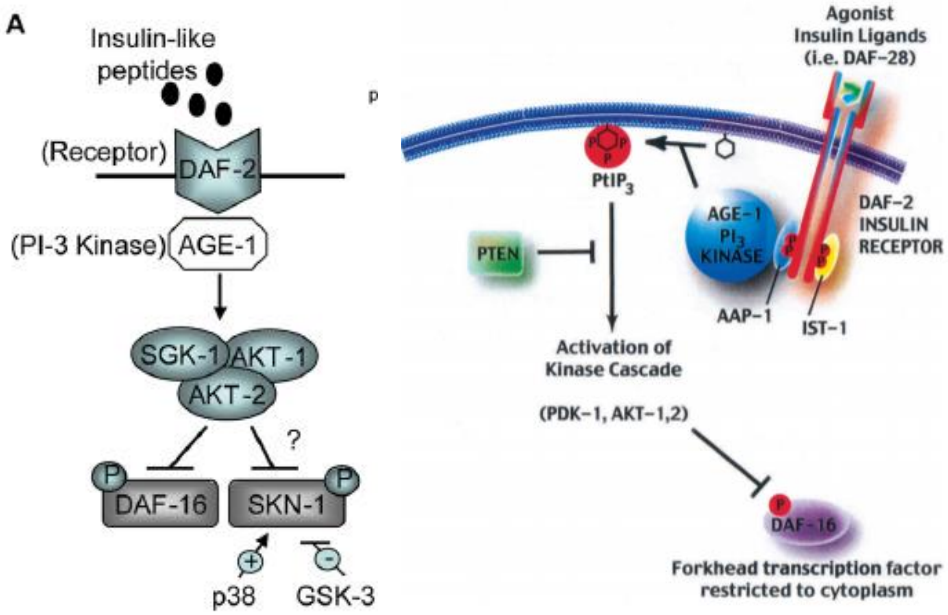

The glycerol-3phosphate dehydrogenase GPDH-1 is also examined as to its relation to ivermectin resistance in this project. The cells upregulate GPDH-1 during hypertonicity (osmotic stress) [40]. Glycerol metabolism is altered in dauer larva, however it appears as if the GPDH-1 homolog is not involved in the IIS under daf-2, suggesting that another GPDH homolog exists [41].

In this project, we observe the effect of mutations in the Skn-1 system on ivermectin sensitivity, including Wdr-23 (inhibitor of Skn-1), Mdt-15 (co-regulator of Skn-1), Mxl-3 (transcription factor related to Skn-1), and Gst-4 (glutathione s-transferase) [42-44]. Wdr-23 works downstream the Daf-2 IIS pathway to bind to Skn-1 and act as a recruiting protein for the proteasome degradation machinery [42]. Mdt-15 acts as a coregulator for certain nuclear receptor transcription factors, including NHR-49, SRB-1 and Skn-1, although its involvement in other stress pathways is not well understood [43, 45]. The basic helix-loop-helix transcription factor Mxl-3 binds to Skn-1 to regulate metabolism and aging/dauer regulation [44, 46]. Gst-4, one of the primary targets of Skn-1, is a glutathione s-transferase that may also be related to a glutathione-dependent prostaglandin D transferase [47, 48]. Gst-4 plays a significant role in regulating oxidative stress in *C. elegans* [35]. In studying various components of the Skn-1 pathway, we hope to have a wide coverage of stress responses in *C. elegans* to determine if they may be related to the *dyf-7* ivermectin resistance pathway.

The other primary type of stress response we wish to analyse are the P-glycoproteins. P-glycoproteins (PGP's) are ABC transporters found across all species, including humans and nematodes [49]. Some nematode PGP's are known to act as efflux pumps, removing toxins from cells. For example, Pgp-3 removes and protects C. elegans from the drugs colchicine and chloroquine and perhaps other related compounds [50], and Pgp-1 and Mrp-1 both contribute to heavy metal resistance [51]. Additionally, a pgp-1::pgp-3 double mutant is sensitive to the bacterial toxin phenazine [52]. Due to their multi-drug resistance properties, we hypothesize that some PGP's are necessary for ivermectin resistance in *dyf* mutants.

6. Methods

6. 1. Gene isolation and genotype confirmation using the polymerase chain reaction

To be able to express *dyf-3* in subsets of sensory neurons and rescue the dye-filling defect cell-autonomously we acquired a set of plasmids with *dyf-3* under the *pCeh-36*, *pDaf-7*, *pGcy-5*, *pGcy-7*, *pKlp-6*, *pOdr-2*, *pSra-6*, *pSre-1*, *pSrh-11*, and *pSrh-142*, a kind gift from Takashi Maruyama and Makoto Koga, Kyushu University. We were able to validate cell-specific *dyf-3* expression in dye-filling neurons by showing that plasmids rescue the dye-filling defect in a *dyf-3* background. To ensure that non-dye-filling neurons were expressing the plasmid-encoded genes, we added to the plasmids *pCeh-36*, *pDaf-7*, *pGcy-5*, *pGcy-7*, *pKlp-6*, *pOdr-2*, *pSra-6*, *pSre-1*, *pSrh-11*, and *pSrh-142* a *gpd-mCherry* sequence after the *dyf-3* cDNA. This should cause the *dyf-3* and *mCherry* to be expressed as an operon, allowing us to use *mCherry* expression as a marker of *dyf-3* expression.

Polymerase chain reaction (PCR) was used to isolate and amplify *mCherry* from the *pUnc-86*. The primers were designed to bind partially to *mCherry* alone in *pUnc-86* and partially to the plasmid that it would later be inserted to. To do this, the annealing temperature for the first 5 cycles out of 40 was set to the portion of the primer that would bind to the gene, and for the last 35 cycles, the annealing temperature of the entire primer was used. All the target plasmids listed above have the same *dyf-3* sequence, therefore the target insertion location for *mCherry* was the same for all plasmids. The *gpd-3* gene was isolated from *pPD4926* by the same means with a sequence added by the designed primers to help it anneal to the target plasmids. All primers for the insertions were designed in the laboratory and ordered from Integrated DNA Technologies.

6.2. Restriction digest

Restriction digest using NcoI enzyme on pCeh-36, pDaf-7, pGcy-5, pGcy-7, pKlp-6, pOdr-2, pSra-6, pSre-1, pSrh-11, and pSrh-142 prepared each plasmid for ligation with *gpd-3* and *mCherry*. The total volume of the preparation was 40 µL: 10 µL plasmid DNA, 3 µL NcoI enzyme,

4 µL NE buffer 4 or cutsmart buffer, and the remaining 23 µL miliQ. The enzyme was added last and the tubes were incubated at 37 °C for 2 hours.

6.3. DNA purification

Two methods were used to purify DNA fragments prior to transformation. The first technique used the Clontech Laboratories Inc. DNA, RNA, and Protein purification kit and the instructions were followed directly.

The other method used to purify plasmid DNA and to yield a higher concentration of fragments was phenol-chloroform extraction followed by ethanol precipitation. All plasmid DNA available (approximately 40 µL of each) was used and miliQ was added for a final volume of 100 µL. A 100 µL of chloroform was added to the diluted DNA and the mixture was vortexed for 1 minute. Next, the solution was centrifuged at max speed for 5 minutes and the aqueous supernatant was removed. Sodium acetate was added to the remaining portion at 1:10 of the total volume, approximately 20 µL. Twice the total volume of 95% ethanol was added (220 µL) and the micture was frozen at -80 °C for 10 minutes. Afterwards, the contents were again centrifuged at max speed for 10 minutes this time, and the ethanol was removed, leaving only the transparent DNA pellet. A final 0.5ml of 70% ethanol was added, centrifuged for 10 minutes, and removed. MiliQ was used (10 µL) to dissolve the DNA pellet. The plasmid DNA was now ready for recombination cloning.

6.4. Cloning using Gibson protocol

DNA fragments *gpd-3*, *mCherry*, and the NcoI-cut plasmid were mixed at ratios such that the total volume was 10 µL DNA to 10 µL Gibson Master Mix. The total content of the fragments was between 0.02-0.5 pmol. The cells were incubated at 50 °C for 60 minutes, then stored at -20 °C prior to transformation.

6.5. Bacterial transformation

On ice, 3 µL of the Gibson recombination product solution was added to thawed DH5-α cells, flicked gently, and incubated on ice for 30 minutes. The bacterial cells plus DNA were transferred to a cold Falcon tube and heat shocked at 42 °C for 90 seconds, then put back on ice for 2 minutes. Next, 1ml SOC medium was added to each Falcon tube and was then incubated for 1 hour in a shaker at 37 °C. Of this solution, 200µl was plated on LB ampicillin for selective growth of transformed colonies. Only large colonies (non-satellite colonies) were picked the following day and used to inoculate LB ampicillin liquid medium in preparation for plasmid extraction.

6.6. Plasmid extraction

Plasmid extraction from bacterial cells was done following the Bio Basic Canada Inc. Molecular Biology kit.

6.7. Outcross strain construction

We made transgenic wild-type controls for each *dyf-3*-complementing strain. The idea was to have wild-type worms that expressed the same transgene as the other strains so that we can confirm that the transgene does not affect the health of the nematode and therefore will not affect its resistance to ivermectin. We made these controls by mating hermaphrodite transgenic worms to male worms of our N2 strain, JD29. The transgenic F1's were mated again to male N2's. Each strain was confirmed as being wild-type for *dyf-3* by performing a dye-filling assay with both DiI and DiO and their mCherry expression and dye-filling was compared to their corresponding transgenic strain.

6.8. Dye-filling of sensory neurons

The worms were washed as described in the egg preparation procedure. Next, 1µl of stock 6mg/ml DiI dye was added to 1000µl of worms in M9 and the tubes were rocked for 1 hour at

approximately 120 revolutions per minute. After the hour, the tubes were centrifuged again to collect the worms so that they could be pipetted onto plates containing *E. coli*. The worms could then be observed under a fluorescent microscope for dye-filling.

Dye-filling using DiO followed a similar procedure, however different concentrations of dye to total solution were used. The DiO stock was 30ng/ml and 9µl was added to 1000µl of solution to create a dark enough staining of the sensory neurons. Additionally, the dye-filled worms were kept on a rocker at maximum speed for 2 hours.

6.9. DNA microinjection

Microinjection procedures were done as described by Mello *et. al.* [53]. We injected each plasmid combination into *C. elegans* strain SP1603, a *dyf-3 (m185)* mutant. All injections were done by Joseph Dent.

6.10. Egg preparation for synchronous growth of C. elegans

To wash the plates, 1ml of M9 buffer was added to the plates containing transconjugant *C. elegans* and allowed to sit for a minute to loosen them from the *E. coli* lawn. Another 0.5ml M9 buffer was added to wash the plates and collect the worms. The solution was added to a 1.5ml tube and was centrifuged for 20 seconds on the lowest speed. Carefully, so as not to disturb the loose *C. elegans* pellet, the supernatant M9 was removed and replaced with 1ml of new M9. The mixture was again centrifuged, the M9 supernatant was removed, and 1ml of new M9 was added. Two hundred fifty microliters (µl) of 2M NaOH and 200µl of bleach were added to the tube and the contents were shaken gently. The tube was allowed to sit for around 8 minutes to allow the adult *C. elegans* bodies to dissolve. The tube was monitored and shaken periodically until digestion was complete, then it was centrifuged at maximum speed for 15 seconds. The supernatant was removed and the pellet was washed 1.5ml M9. A final volume of 200µl M9 was added to the final pellet. The eggs were plated onto a bacteria-free LB plate so that the hatching larvae would be starved and would enter the dauer stage.

6.11. Ivermectin Assay

Plates containing ivermectin were prepared similarly to standard NGM plates with the addition of 0.5% DMSO and the desired ivermectin concentration after the agar cooled following autoclave sterilisation. Plates of 0.01, 1, 2, 5, 10, and 20ng/ml were used in these assays.

The strains to be tested were prepared for synchronous growth. After 24 hours of plating synchronised eggs on empty NGM plates, the established dauers were washed off. For strains with a transgenic marker, approximately 100 larvae were plated onto each concentration of ivermectin plates 4 times (4 trials for each concentration). For strains without a transgene, only 50 larvae were placed on each plate since 100% of these worms were expressing the desired phenotype. The plates were stored in a 20°C incubator for 72 hours, then the gravid (fertile) adults were counted for the percent survival.

6.12. Salt chemotaxis assay

Chemotaxis plates were prepared with salt concentrations of 5mM KP6, 1mM $MgSO_4$, 1mM CaCl and 2% agar and 10ml solution was poured into 10cm in diameter petri plates. The origin of the plates was labeled with a diameter of 0.5cm. Additionally, a circle 2cm in diameter was marked at one end for the test area and at the exact opposite end for the control area. A salt plug containing 5mM KP6, 1mM $MgSO_4$, 1mM CaCl, and 50mM NaCl was placed in center of the test area the night before the assay to allow a salt gradient to form. A control plug with the same concentration as the test plate (5mM KP6, 1mM $MgSO_4$, 1mM CaCl) was placed in the center of the control area also the night before. All plates were prepared the day before the assay.

The strains involved in the salt chemotaxis assay were synchronized using the egg preparation method described above. The synchronized worms grew for 48 hours, at which point they were at the young adult stage. The worms were washed three times in salt chemotaxis buffer (5mM KP6, 1mM $MgSO_4$, 1mM CaCl) and approximately 100 worms were placed at the center of the assay plates and excess liquid was sopped up with a kimwipe. Immediately after dropping the worms, 2µl of 1M sodium azide was dropped onto each salt plug. The plates were then left in

a 20°C incubator for 1 hour and then were immediately transferred to a 4°C fridge for 48 hours. After this, the plates were counted.

6.13. Electropharyngiogram (EPG) Assay

To confirm the genotype of strains containing the *eat-4 (ky5)* mutation, an EPG was performed. The procedure was performed as described by Li et. al. 1997, with the exception of using intact, live worms for the assay. [54]

6.14. Statistics

For the ivermectin dose response assays, we use IGOR Pro (WaveMetrics Inc.) MATLAB (Mathworks) to generate dose response curves and statistical analysis respectively. Joseph Dent created a program to run a jackknife analysis on the dose response data. A jackknife is a type of bootstrap where the same curve function is generated many times, and each time one different data point is removed from the set once. We used a jackknife because even though we had 4 plates per strain, per concentration, this only generated one curve with one EC50 value. With this type of analysis, we have 24 different curves using the same data set, which generates an error based on what the curve looks like without each data point. We then used a one-tailed t-test to compare the average EC50 values to determine significance.

7. Results

7.1. *C. elegans* strains with complemented *dyf-3* in the sensory neurons

The plasmids in Table 1 were constructed to be injected into a *dyf-3* knockout background to rescue Dyf-3 function in certain subsets of sensory neurons. We co-express the mCherry tag under the same promoter to confirm *dyf-3* expression in the target neurons. To ensure these two proteins are expressed separately and fold correctly, we add the SL2 trans-splicing target sequence *gpd-2 and gpd-3* between *dyf-3* and *mCherry*. *Gpd-2* and *gpd-3* constitute an operon that encodes isoforms of a glyceraldehyde-3-phosphate dehydrogenase (GAPDH) and has been shown to be a target of the SL2 mRNA trans-splicing event [55]. Including the *gpd-2,3* intergenic sequence in the construct between *dyf-3* and *mCherry* ensures that even when expressed under the same promoter, the two mRNAs are separated and the proteins fold correctly. Plasmids modified with the *gpd-2,3* and the *mCherry* sequence were extracted from the bacterial cells and injected into the *dyf-3* knockout mutant strain SP1603(*m185*) along with a second plasmid, the transformation marker, that would express GFP under control of the (*ofm-1p*) reporter in coelomocytes. In some cases, three plasmids, including the GFP reporter plasmid, were injected into the same worm to create a larger subset of rescued sensory neurons. All the constructed strains with these plasmids are shown in Table 2.

Table 1. Lists the plasmids constructed containing *dyf-3::gpd-3::mCherry* under various promoters. The table also shows which sensory neurons are expected to be rescued under each promoter. The sensory neurons written in red are the ones that are exposed to the external environment and dye-fill in wild-type nematodes.

Promoter	Construct	Expresses in	Dye-fills?
Ceh-36p	ceh-36p::dyf-3::gpd-3::mCherry	ASE	No
Daf-7p	daf-7p::dyf-3::gpd-3::mCherry	ASI, ADE	Yes
Gcy-5p	gcy-5p::dyf-3::gpd-3::mCherry	ASE right	No
Gcy-7p	gcy-7p::dyf-3::gpd-3::mCherry	ASE left	No
Klp-6p	klp-6p::dyf-3::gpd-3::mCherry	IL2	No
Odr-2p	odr-2p::dyf-3::gpd-3::mCherry	IL2, ASG	No
Sra-6p	sra-6p::dyf-3	ASH, ASI	Yes
Sre-1p	sre-1p::dyf-3	ADL, ASJ	Yes
Srh-11p	srh-11p::dyf-3::gpd-3::mCherry	ASJ	Yes
Srh-142p	srh-142p::dyf-3::gpd-3::mCherry	ADF	Yes

To validate the proper cell-specific expression of *dyf-3* and the rescue of sensory cilia defects, we examined the mCherry expression and/or dye-filling as appropriate. Figures 16-24 show images of each constructed strain with their *mCherry* expression and their ability to dye-fill when exposed to DiO, a green fluorescent dye. Most strains with mCherry appear to express the red fluorescent tag without complication.

Table 2. Shows the strains constructed through microinjection and indicates whether those rescued sensory neurons were expected to dye-fill and if dye-filling was observed in that strain. The boxes filled in yellow highlight discrepancies between predicted dye-filling phenotype and what was observed when the strains were tested.

Strain	Genotype	Expected to Dye-fill?	Dye-fills with DiI/DiO
JD663	dyf-3(m185) IV; vuEx297[sra-6p::dyf-3, sre-1p::dyf-3, ofm-1p::GFP]	Yes	Yes
JD684	dyf-3(m185) IV; vuEx298[sra-6p::dyf-3, ofm-1p::GFP]	Yes	No
JD685	dyf-3(m185) IV; vuEx299[sre-1p::dyf-3, ofm-1p::GFP]	Yes	Yes
JD686	dyf-3(m185) IV; vuEx300[klp-6p::dyf-3::gpd-3::mCherry, ofm-1p::GFP]	No	No
JD687	dyf-3(m185) IV; vuEx301[daf-7p::dyf-3::gpd-3::mCherry, ofm-1p::GFP]	Yes	Yes
JD688	dyf-3(m185) IV; vuEx302[ceh-36p::dyf-3::gpd-3::mCherry, ofm-1p::GFP]	No	No
JD689	dyf-3(m185) IV; vuEx303[srh-142p::dyf-3::gpd-3::mCherry, ofm-1p::GFP]	Yes	No
JD690	dyf-3(m185) IV; vuEx304[srh-11p::dyf-3::gpd-3::mCherry, ofm-1p::GFP]	Yes	No
JD691	dyf-3(m185) IV; vuEx305[odr-2p::dyf-3::gpd-3::mCherry, ofm-1p::GFP]	No	Yes
JD692	dyf-3(m185) IV; vuEx306[gcy-5p::dyf-3::gpd-3::mCherry, gcy-7p::dyf-3::gpd_mCherry, ofm-1p::GFP]	No	No
JD693	dyf-3(m185) IV; vuEx307[ofm-1p::GFP]	No	No
JD694	vuEx298[sra-6p::dyf-3, ofm-1p::GFP]	Yes	Yes
JD695	vuEx299[sre-1p::dyf-3, ofm-1p::GFP]	Yes	Yes
JD696	vuEx300[klp-6p::dyf-3::gpd-3::mCherry, ofm-1p::GFP]	Yes	Yes
JD697	vuEx301[daf-7p::dyf-3::gpd-3::mCherry, ofm-1p::GFP]	Yes	Yes
JD698	vuEx302[ceh-36p::dyf-3::gpd-3::mCherry, ofm-1p::GFP]	Yes	Yes
JD699	vuEx303[srh-142p::dyf-3::gpd-3::mCherry, ofm-1p::GFP]	Yes	Yes
JD700	vuEx304[srh-11p::dyf-3::gpd-3::mCherry, ofm-1p::GFP]	Yes	Yes
JD701	vuEx305[odr-2p::dyf-3::gpd-3::mCherry, ofm-1p::GFP]	Yes	Yes
JD702	vuEx306[gcy-5p::dyf-3::gpd-3::mCherry, gcy-7p::dyf-3::gpd_mCherry, ofm-1p::GFP]	Yes	Yes
JD703	vuEx307[ofm-1p::GFP]	Yes	Yes
JD704	vuEx297[sra-6p::dyf-3, sre-1p::dyf-3, ofm-1p::GFP]	Yes	Yes

Interestingly, not all strains dye-filled as expected (summarised in table 2). In the case of JD684 (expected to rescue the ASH and ASI sensory neurons), the strain would express GFP but not dye-fill, although JD663 (expected to rescue the ADL, ASJ, ASH, and ASI sensory neurons) does appear to rescue and dye-fill both ASH and ASI. This suggests that perhaps JD684 acquired *ofm-1p* and not *sra-6p* during microinjection. This would make the worms express GFP but not complement *dyf-3* in any sensory neurons, which is what was observed in the dye-filling assay. We are working on re-injecting both the *sra-6p* construct and *ofm-1p* into a *dyf-3* background. If we cannot obtain a strain that expresses GFP and rescues dye-filling, then the two plasmids may not be compatible within *C. elegans*.

Another unexpected event was that two strains, JD689 and JD690 (expected to rescue *dyf-3* in ASJ and ADF respectively), should have dye-filled in the rescued neuron but did not (see figures 22 and 23). The mCherry expression in both strains appears to be as anticipated, with one set of sensory neurons expressing the marker, therefore we expected to see dye-filling of the rescued sensory neurons. The reason for the lack of dye-filling is currently unknown. Perhaps the *srh-142p* and *srh-11p* rescued *dyf-3* in a subset of sensory neurons other than the ones stipulated in the literature, particularly sensory neurons that do not dye-fill. Both these strains displayed ivermectin resistance levels similar to that of SP1603(*m185*) ($p<0.005$), supporting the hypothesis that the *dyf-3*-expressing sensory neurons are not involved in ivermectin sensitivity.

In contrast to the unexpected lack of dye-filling in JD689 and JD690, the plasmid *odr-2p::dyf-3::mCherry* in the strain JD691, which was expected to express only in non-dye-filling neurons, including the IL2 and ASG sensory neurons, nevertheless rescued two pairs of dye-filling sensory neurons, shown in appendix figure 5. The mCherry expression in this strain is very widespread via the broad expression of the *odr-2p* promoter, however none of the known cells that express under this promoter were thought to be dye-filling sensory neurons. Of the two pairs of sensory neurons that dye-filled, only one of these pair of neurons appeared to express mCherry. If a sensory neuron has rescued Dyf-3 function but does not express mCherry, then either the SL2 transplicing event is not occurring and the Dyf-3 protein folds correctly but not mCherry, or Dyf-3 expression is not always cell-autonomous and one cell's Dyf-3 rescues cilia function in another neuron. Otherwise, a level of expression that is insufficient to be able to see mCherry may nevertheless be sufficient to rescue *dyf-3*.

Figure 11. Sensitivity of cell specific *dyf-3* rescue strains to ivermectin. (A) Shows the ivermectin EC50 values of various *dyf-3* rescue strains. The first two grey bars show median EC50 values in ng/ml for non-transgenic wild type (left) and *dyf-3* mutant (right) controls. For each transgene, the blue bar shows the EC50 of the transgene in a *dyf-3* mutant background and the red bar shows the EC50 value for the same transgene in a wild type background ($p<0.005$). The neurons expected to express the *dyf-3*-rescuing transgene are shown below the bars and the neurons that dye-filled in these experiments are indicated in red. (B) Shows the ratio of EC50 values of (*dyf-3*- background with construct):(wild-type background with construct) strains The sensory neurons rescued/overexpressed are written below each bar, with the sensory neurons in red indicating sensory neurons that dye-filled when rescued ($p<0.01$). Sensory neurons written in black did not dye-fill when rescued. The value of each ratio is given above each bar. (C) Shows the predicted linear correlation between the number of dye-filling sensory neurons and their resistance to ivermectin in terms of the EC50. (D) Shows two strains that we re-tested for ivermectin sensitivity after the wild-type was re-thawed and (E) shows their corresponding ratios to their outcross counterparts ($p<0.012$).

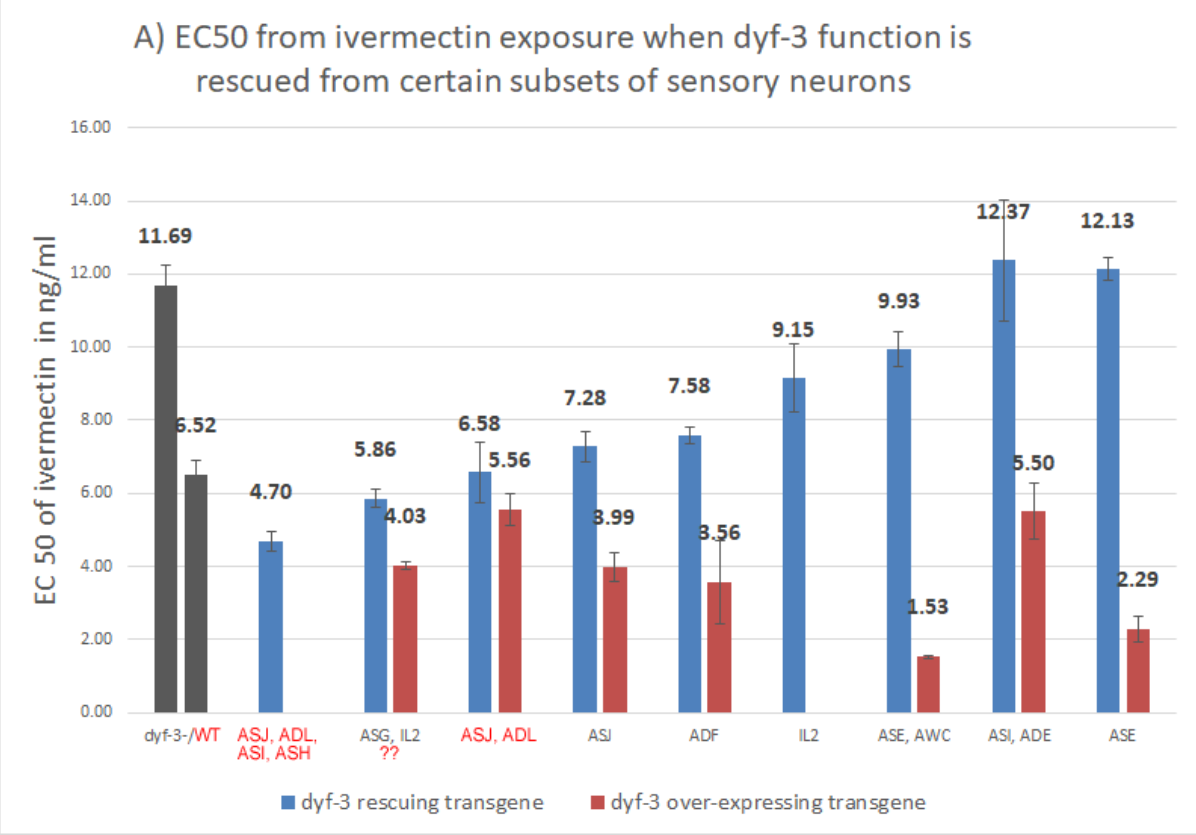

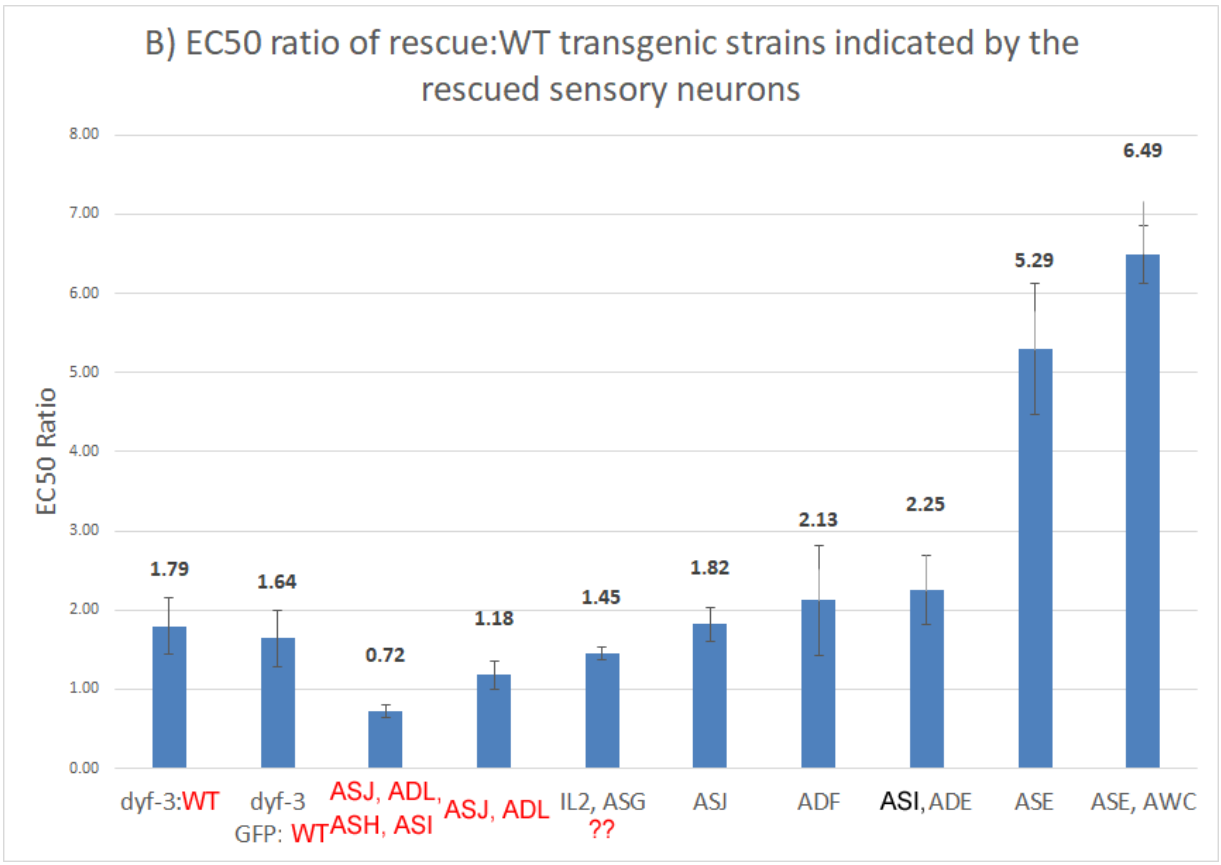
B) EC50 ratio of rescue:WT transgenic strains indicated by the rescued sensory neurons
EC50 Ratio
8.00
7.00
6.00
5.00
4.00
3.00
2.00
1.00
0.00
1.79
1.64
0.72
1.18
1.45
1.82
2.13
2.25
5.29
6.49
dyf-3:WT
dyf-3 GFP: WT
ASJ, ADL, ASH, ASI
ASJ, ADL
IL2, ASG ??
ASJ
ADF
ASI, ADE
ASE
ASE, AWC

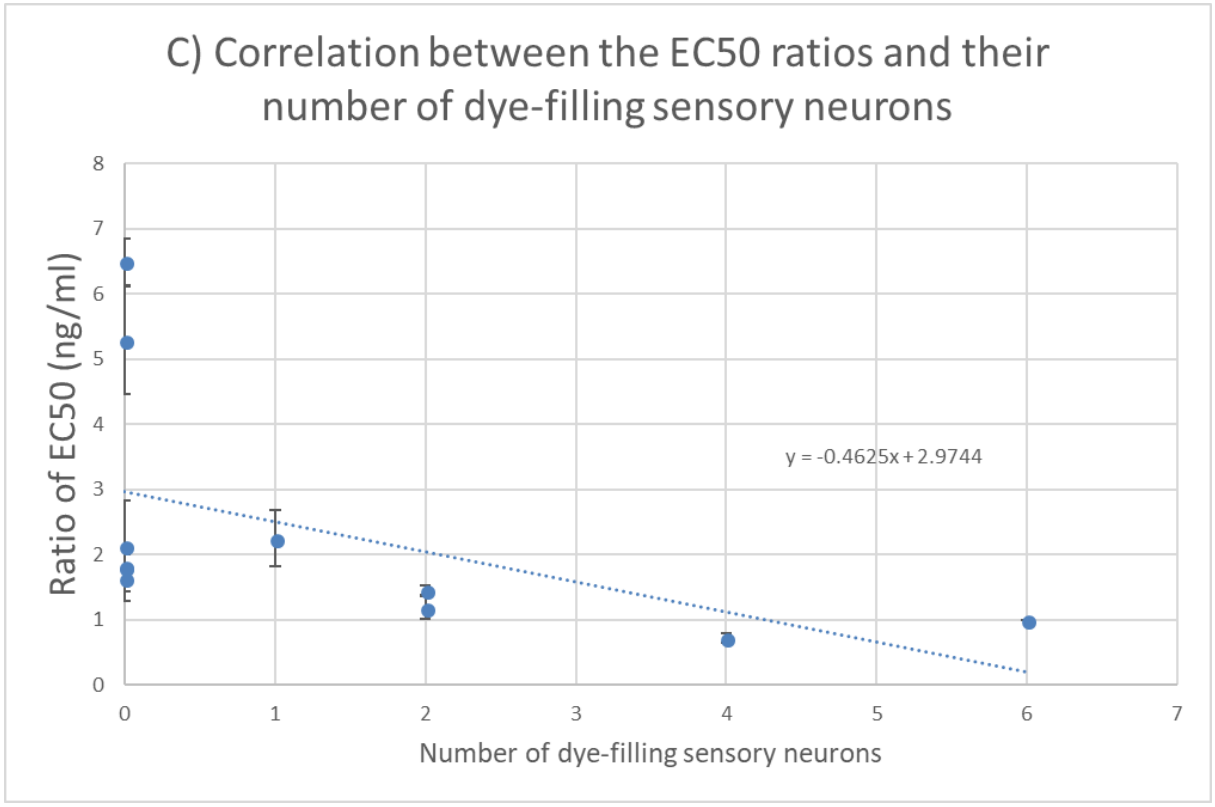
C) Correlation between the EC50 ratios and their number of dye-filling sensory neurons
Ratio of EC50 (ng/ml)
8
7
6
5
4
3
2
1
0
y = -0.4625x + 2.9744
0
1
2
3
4
5
6
7
Number of dye-filling sensory neurons

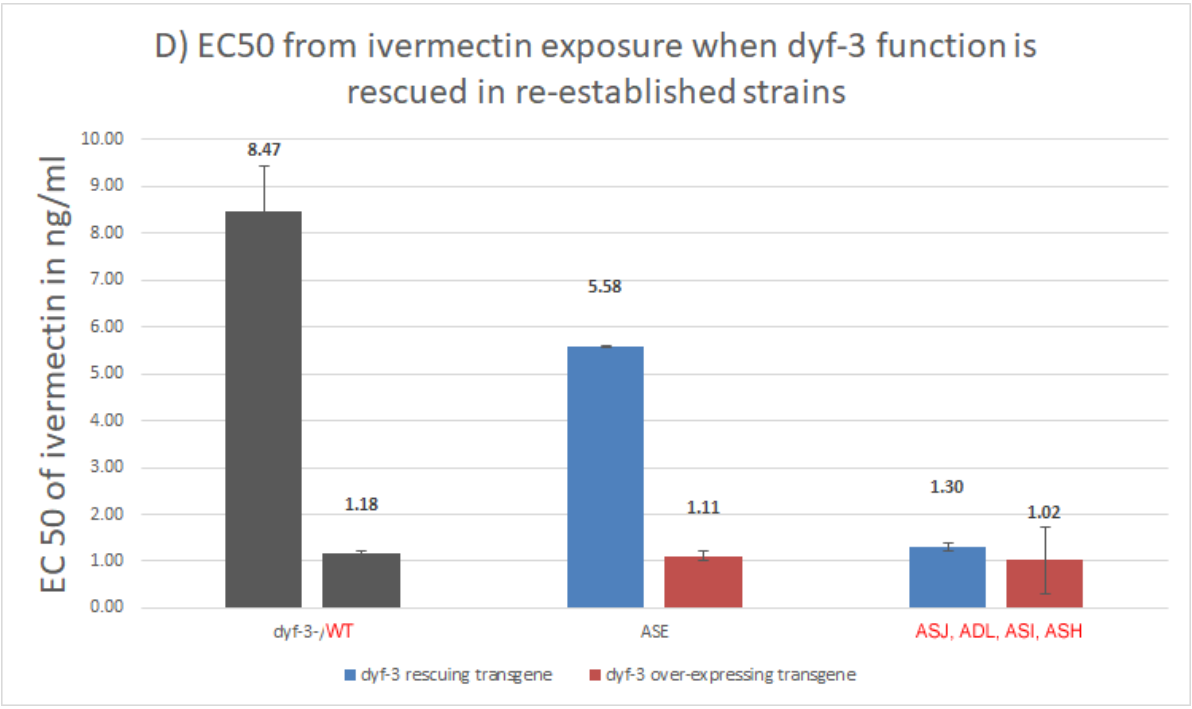

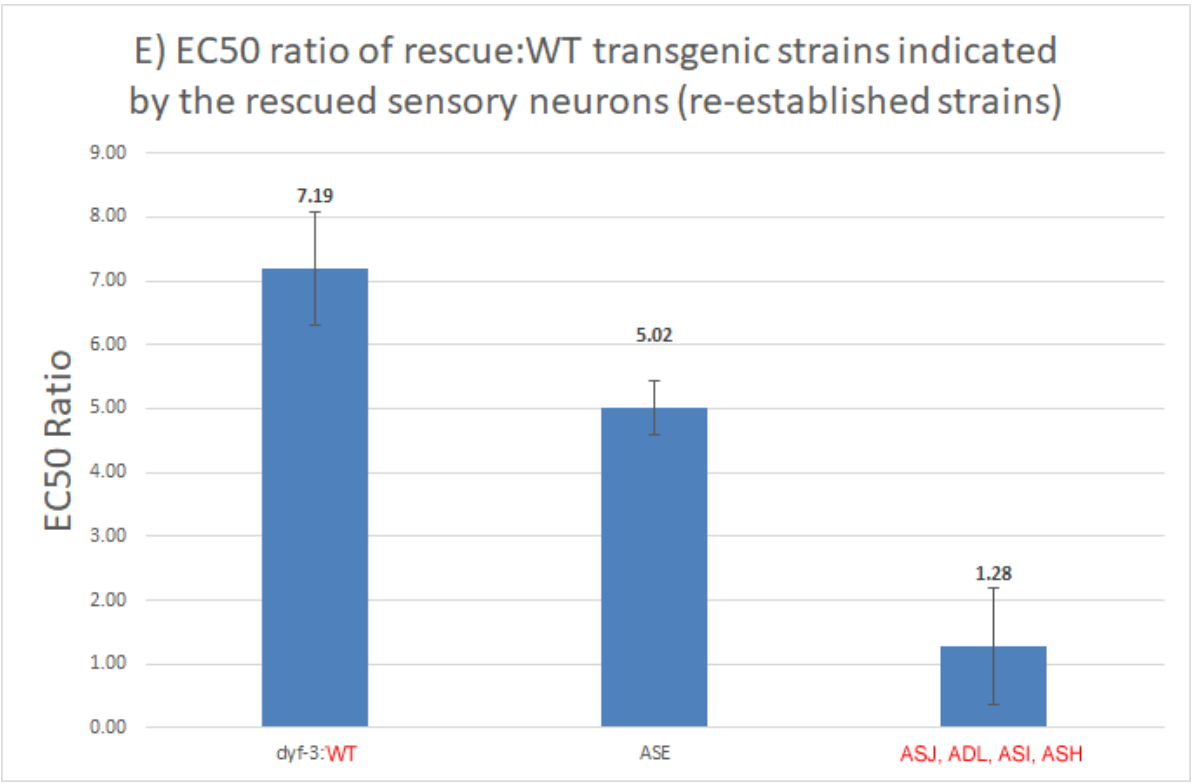

Figure 11A shows the results from the ivermectin dose-response assay's in the *dyf-3* rescue strains. We generated dose-response curves for each strain and used the EC50 (dose of drug that

prevents 50% of the population from reaching fertile adulthood after 3 days) as a measure of ivermectin resistance. We then used a jackknife analysis to determine the standard error for each EC50. We compared the ratio of each strain with a corresponding outcross strain, which is a wild-type strain that expresses the transgene. The outcross strains serve as controls for effects of the transgene on growth independent of the effects on ivermectin sensitivity. If the constructs do not affect the nematodes' health in a wild type background, then we expect their EC50 to ivermectin to be similar to that of the wild-type strain.

This was the case for all strains except for JD698 (over-expresses Dyf-3 in the ASE neurons) and JD702 (over-expresses Dyf-3 in the ASE and AWC neurons). JD698 had an EC50 for ivermectin of 1.53 ng/mL, which is significantly lower than that of the wild-type EC50 at 6.52 ng/mL ($p<0.05$). The EC50 of JD702 was also significantly lower at 2.29 ng/mL ($p<0.05$). What stands out in both strains is that both over-express *dyf-3* in the ASE sensory neurons, which are responsible for chemotaxis towards salt and other chemicals. To rule out the possibility that over-expressing the transgene makes the worms sick through non-functional ASE neurons, we performed a sodium chemotaxis assay with the results shown in Figure 12. Statistically, JD702 (over-expresses *dyf-3* and *mCherry* in ASE only) has chemotaxis behaviour similar to that of the wild-type and JD698 (over-expresses *dyf-3* and *mCherry* in ASE and AWC) does not ($p<0.01$), however the wild-type worms that do not express the transgene in JD698 also have an abnormal chemotaxis index (CI). This indicates that something else is making this strain ill independent from ivermectin.

These results also suggested that our wild-type strain may not be truly wild-type so we re-thawed JD29 and generated some new outcross strains (using the fresh JD29) and re-tested these strains for ivermectin sensitivity. Based on our results, shown in Figure 11D and 11E, we confirmed that there was an issue with our N2 strain and that new outcrosses would need to be established for all strains. When these strains are obtained, these ivermectin assays should be repeated.

Figure 12. Shows the chemotaxis index of the transgenic strains exhibiting high ivermectin sensitivity in a wild type background. JD29 (our wild type strain) acts as the positive control and PR679 and OH3679 are two negative control strains (*che-1(p679)* and *che-1(ot151)*), both of which have ASE deficiencies. The worms that expressed the *dyf-3::mCherry* transgene were counted the in red bars whereas the worms without a transgene are counted in black ($p<0.01$).

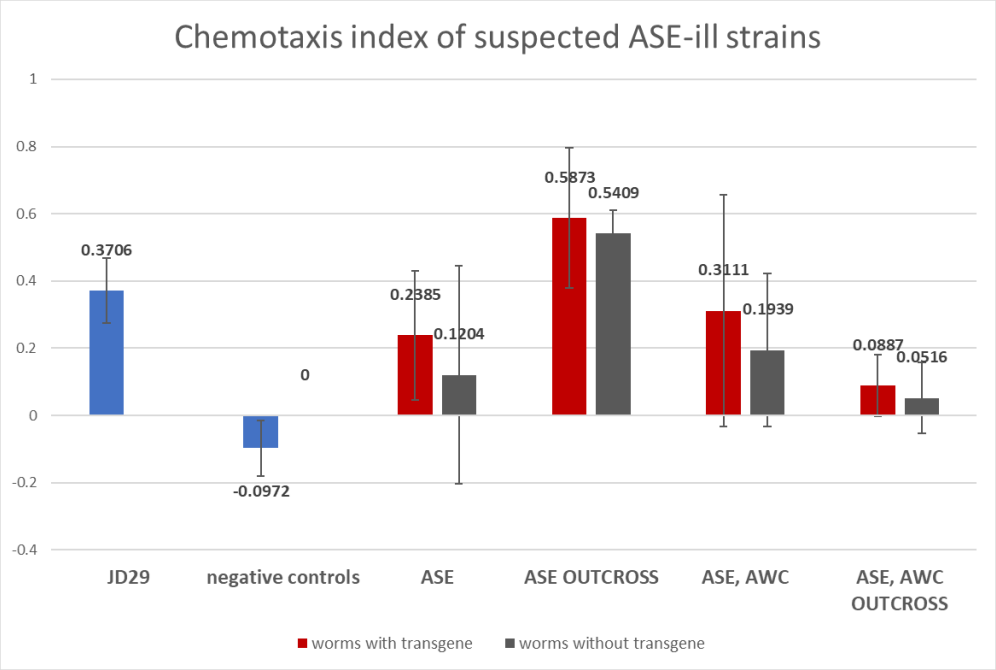

Figure 11B shows the ratios of EC50 of each strain to their corresponding outcrossed strain to control any effect the transgene may have on a given strain. If a transgene has no effect of ivermectin sensitivity, then the ratio of the EC50 for the same transgene in a wild type background and a dyf-3 background should be equal to the ratio of wild type to the *dyf-3* mutant strain, which is ~1.8. In contrast, if the transgene completely rescues the ivermectin sensitivity in the *dyf-3* mutant background, then the EC50 of the transgenic strain should be equal to the EC50 of the wild type and the ratio should be 1.0. Intermediate ratios indicate intermediate levels of rescue.

Based on our ivermectin assays, the most resistant strain was JD687, which rescues *dyf-3* function in ASI and ADE (EC50 ratio of 2.25 versus 1.79 for *dyf-3*-:WT). ASI normally dye-fills and we did see this in the dye-filling assay (see figure 17), however the *daf-7p* did not consistently rescue dye-filling in ASI.

Interestingly, the *srh-11p* and *srh-142p* appear to express mCherry in one subset of sensory neurons as expected, (ASJ and ADF) but do not dye-fill. Whether ASJ and ADF are expressing *dyf-3* in these strains is not clear because dye-filling was not rescued, however, we have not confirmed that the mCherry-expressing neurons are ASJ and ADF and the transgenes might be expressed elsewhere. In this case, a better imaging technique would be helpful to more accurately identify the sensory neurons.

The most sensitive strains are JD663 (rescues *dyf-3* in ASJ, ADL, ASH, and ASI), JD685 (rescues ASJ and ADL), and JD691 (expected to rescue ASG and IL2), with the most sensitive being the strain that rescues four subsets of dye-filling sensory neurons (EC50 ratio of 0.72). The next two most sensitive strains, JD685 (EC50 ratio of 1.18) and JD691 (EC50 ratio of 1.45), both rescue dye-filling in two subsets of sensory neurons. If dye-filling sensory neurons contributed additively to ivermectin resistance, then we would expect to see similar EC50 values between these two strains. Indeed, both strains have an EC50 value similar to that of the wild-type in these experiments ($p<0.005$), however the ratio of the rescue strain to its outcross is higher than that of the wild-type, suggesting that the transgenes affect ivermectin sensitivity to some degree ($p<0.01$).

Furthermore, one of the sensitive strains, JD691, was not expected to rescue dye-filling sensory neurons (discussed previously, see figure 20) but did. We expected the *odr-2p* to express *dyf-3* and *mCherry* in ASG and IL2 and it is known to express in several interneurons including AIB, AIZ, RME, SMB, etc. [56]. It's possible that some Dyf-3 was somehow able to travel to adjacent, non-*dyf-3* expressing neurons during development. We already know that expression in IL2 does not rescue dye-filling sensory neurons through the JD686 strain, which rescues IL2 only, so the ivermectin sensitivity likely is the result of *dyf-3* expression in the dye-filling neurons. Most likely the dye-filling sensory neurons are rescued by leaky, or previously undocumented, expression of *dyf-3* from the *odr-2p* promoter. JD686 has an EC50 from ivermectin of 9.93 ng/ml, which is an intermediate resistance level between wild-type and the *dyf-3* mutant ($p<0.005$), which is consistent with *dyf-3* rescue in a subset of dye-filling sensory neurons.

The aim of these experiments was to establish a correlation between the functionality of the dye-filling sensory neurons and the resulting strains' decreasing resistance to ivermectin.

Figure 11C shows the suggested correlation. Based on our results, *C. elegans* becomes more sensitive to ivermectin as we restore the cilia function in an increasing number of dye-filling sensory neurons, whereas restoring cilia function in non-dye-filling neurons has little or no effect (correlation coefficient = 0.46).

7.2. Interneuron communication mutants in *C. elegans*

If dye-filling defective mutants are resistant because the sensory neurons are not receiving sensory input, which in turn triggers a stress response, then preventing the sensory neurons from communicating with the rest of the organism should have a similar sensitivity to ivermectin as the *dyf* mutants. We searched Wormatlas (http://www.wormatlas.org/) for genes involved in neurotransmission and that are expressed in amphid sensory neurons and identified (list genes) candidates. We obtained strains with putative loss-of-function alleles for each gene and tested them for ivermectin sensitivity. The ivermectin EC50 values obtained for these strains are shown in Figure 13. Individually, the mutant strains are not resistant to ivermectin. In fact, mutations in *eat-4*, *inx-7* and *unc-31* make the nematode more sensitive to ivermectin than the wild type ($p<0.01$). This indicates that a lack of the Inx-7 gap junction, glutamatergic neurotransmission (Eat-4), or dense core vesicle release (Unc-31) likely makes the nematodes generally more sickly and more susceptible to ivermectin.

Figure 13. Shows the EC50 values obtained from various interneuron communication mutants to ivermectin through assays done by Katia Fox. The EC50 values for each strain are displayed above each bar ($p<0.01$).

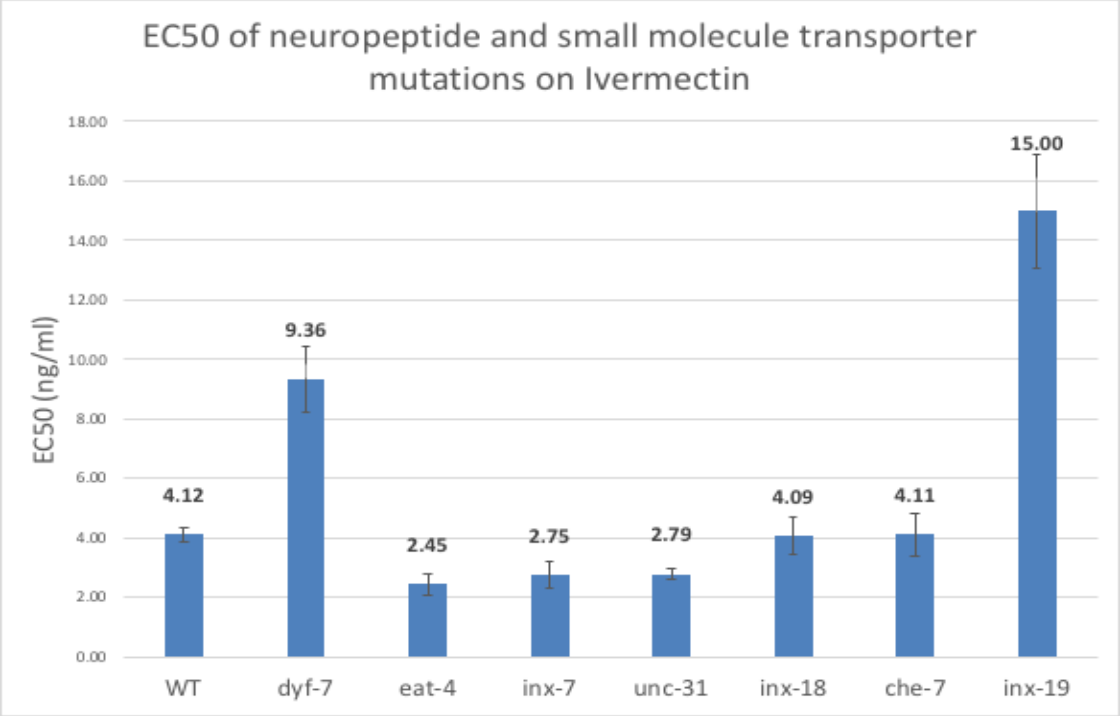

The *inx-19(ky634)* mutant stands out because it is more resistant to ivermectin than *dyf-7*. This result prompted us to check the dye-filling phenotype of all the neurotransmission defective strains. Only the *inx-19* strain shares the dye-filling defective phenotype of *dyf-7*. This finding suggests that Inx-19 plays a role in ivermectin resistance but that the resistance could be caused by the dye-filling defect rather than the neurotransmission defect in the inx-19 mutant.

7.3. Stress response mutants and ivermectin resistance in C. *elegans*

In the final portion of this project, we wanted to determine if certain nematode stress response pathways are involved in ivermectin resistance. The first stress response pathway we examined was the P-glycoprotein (PGP)-mediated efflux pathway. Because there are over 20 PGP genes in C. elegans [49] and because they are thought to have overlapping substrate specificities, we thought they might have redundant ivermectin efflux properties. Therefore we focused on the class of PGP genes that show the greatest similarity to efflux pumps known to be involved in drug efflux and we created the quintuple efflux pump mutant strain, JD662 (*pgp-1(pk17)::pgp-*

2(gk114)::pgp-3(pk18)::pgp-9(tm830)::mrp-1(pk89). We compared JD662 to a strain with the same PGP mutations plus the *dyf-7(m537)* mutation to determine if the PGP genes are necessary for the *dyf-7* mediated ivermectin resistance (i.e. epistasis). The results from the ivermectin assays are shown in Figure 14. If any subset of the PGP mutations were necessary for *dyf-7*-mediated ivermectin resistance, then we would expect the *dyf-7-pgp-1(pk17)::pgp-2(gk114)::pgp-3(pk18)::pgp-9(tm830)::mrp-1(pk89)* mutant to have a similar EC50 to that of the *pgp-1(pk17)::pgp-2(gk114)::pgp-3(pk18)::pgp-9(tm830)::mrp-1(pk89).* In this case, JD712 (*pgp-1(pk17)::pgp-2(gk114)::pgp-3(pk18)::pgp-9(tm830)::mrp-1(pk89)::dyf-7(m537)*) displayed intermediate ivermectin sensitivity between that of the wild-type strain and the *dyf-7* mutant but was closer to wild type with an EC50 of 4.63 ng/ml ($p<0.005$). This indicates that one or more of the P-glycoproteins/multi-drug-resistant proteins removed are necessary for ivermectin resistance through *dyf-7* and are therefore part of the resistance pathway. We are currently constructing strains with various subsets of these PGP's to determine which ones may be a part of the *dyf-7* resistance pathway.

Figure 14. Shows the EC50 to ivermectin of the quintuple mutant JD662 (*pgp-1(pk17)::pgp-2(gk114)::pgp-3(pk18)::pgp-9(tm830)::mrp-1(pk89)*) and its *dyf-7* double mutant JD712 (*pgp-1(pk17)::pgp-2(gk114)::pgp-3(pk18)::pgp-9(tm830)::mrp-1(pk89)::dyf-7)m537)*). The mean EC50 for each strain is shown above each bar ($p<0.005$).

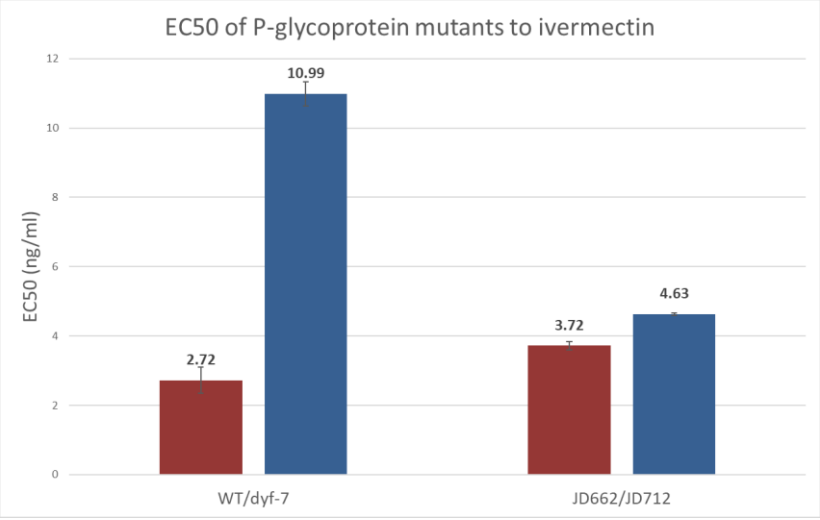

In addition to the PGP mutants, we tested mutants that have reduced or enhanced activity of upstream regulators of various stress pathways. We studied loss-of function mutations in the

FOXO transcription factor Daf-16 (necessary for the dauer response), the heat-shock transcription factor Hsf-1, and a marker of osmotic stress, GPDH-1. Their dose response to ivermectin are shown in Figure 15. All three mutants, when paired with *dyf-7*, were more sensitive than *dyf-7(m537)* alone ($p<0.005$), indicating that each pathway may assist in detoxifying ivermectin or that the mutants are generally less healthy and therefore more drug sensitivity. Interestingly, the *daf-16* and *hsf-1* mutants show a similarly increased sensitivity to ivermectin when paired with *dyf-7*. This may simply be due to the added burden that the lack of this stress response incurs on *C. elegans*. However, even the *daf-16;dyf-7* and *hsf-1;dyf-7* mutants are significantly more sensitive to ivermectin than wild type, indicating that these stress pathways play a small role in dyf-7-mediated resistance.

Figure 15. Shows the EC50 to ivermectin of three stress response mutants, with the mean EC50 shown above each bar. Each stress response mutant has a *dyf-7* double mutant counterpart for establishing the epistatic relationship between the two genes. These ivermectin assays were performed by Katia Fox (unpublished data).

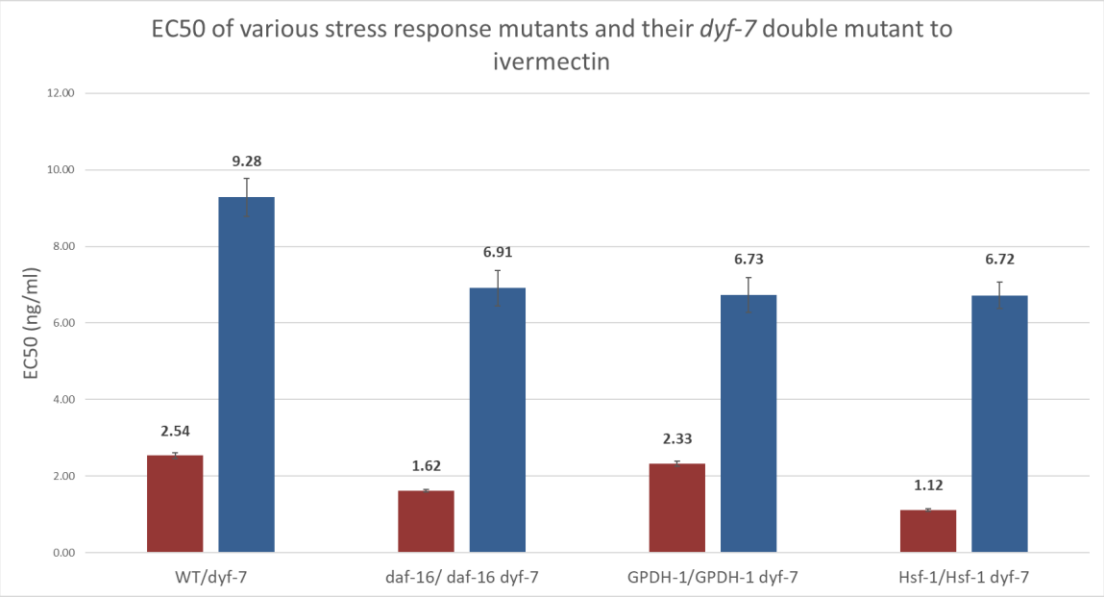

We wished to test other stress response genes, such as those interacting with the Skn-1 transcription factor (Wrd-23, Mxl-3, Mdt-15, Gst-4, and Skn-1 itself) and all the *C. elegans* PGP's in their involvement in the *dyf-7* ivermectin resistance pathway. Unfortunately, a lack of time prevented us from acquiring all *dyf-7* double mutants so their ivermectin assays were not done. We are particularly interested in the PGP mutants because of the preliminary data from this project,

but also the Skn-1-related mutants since Skn-1 regulates all three phases of *C. elegans* stress responses [35].

The Skn-1-related mutants were tested for dye-filling. All mutants dye-filled with DiI except RB1823, the *gst-4(ok2358)* mutant. The *gst-4(ok2358)* is a deletion mutation that also removes the adjacent *msp-38* gene (encodes a major sperm protein). When RB1823 was outcrossed to the N2 strain twice, the new strain regained the ability to dye-fill. We named this new strain JD741. The gene that was causing the defect in dye-filling has yet to be identified, although we are certain that it was not the *gst-4* or *msp-38* mutations.

8. Discussion

8.1. *C. elegans* sensory neuron *dyf-3* complementation

The aim of the first portion of this project was to determine whether the *dyf* genes confer ivermectin resistance by modifying the drug permeability properties of sensory neurons, or if they confer resistance by inhibiting signaling of sensory neurons with specific modalities. In the former case, we predicted that rescuing cilia defects in the *dyf-3* mutant in any subset of dye-filling neurons would increase ivermectin sensitivity whereas rescuing *dyf-3* in non-dye-filling neurons would have no effect. In the latter case we predicted that rescuing the cilia defects only in specific sensory neurons would rescue ivermectin sensitivity. Our data suggests that rescuing at least 2 dye-filling sensory neurons is sufficient to make C. elegans as sensitive to ivermectin as the wild-type ($p<0.005$), although this may not hold true when we re-examine each strain with the re-thawed N2 strain. If the wild-type EC50 to ivermectin is closer to 1.18 ng/ml and the test strain EC50's are similar to what we have already found, then even rescuing 4 dye-filling sensory neurons will only relay intermediate sensitivity.

Initially, it appeared as if rescuing the cilia of four dye-filling sensory neurons (ASJ, ADL, ASI, and ASH) rendered the strain slightly more sensitive to ivermectin than the wild-type ($p<0.005$). This finding seems unusual, therefore we questioned the validity of our N2 strain at the time and since re-thawed and re-tested the strain. Indeed, when it was re-tested, the EC50 to ivermectin came down to 1.18 ng/ml and that of JD663 to 1.30 ng/ml, which are statistically different but very close in value ($p<0.012$). The N2 strain may have developed over time a mutation that made it somewhat more resistant to ivermectin. This would explain why in the data in earlier experiments the EC50 of JD29 is lower than 6.52 ng/ml (between 2.5-4 ng/ml). Despite the issue with the N2 strain, we should still be able to compare the EC50 values of the tested strains against the new N2 EC50, shown in figure 11D.

We determined that rescue of the dye-filling phenotype in the ASJ and ADL sensory neurons (in JD685), as well as rescue of a pair of unidentified sensory neurons (in JD691), are sufficient to make the nematode susceptible to drug. We are uncertain which sensory neurons were

rescued in JD691 since we did not expect to see any dye-filling. We determined if the rescued neurons were expressing mCherry by overlapping the images of the mCherry-expressing neurons and the DiO-filled neurons in the same worm. The issue with this is that the worms were not completely paralysed (polyurethane beads were used to keep the worms alive and neurons intact) and could still move incrementally, which would affect the position of its neurons. Additionally, this strain expresses mCherry in many interneurons that are closely positioned to the sensory neurons, making it difficult to distinguish the various neuron types. More advanced imaging techniques would be useful for accurately identifying the sensory neurons, such as taking both lateral and ventral-dorsal views of completely immobile worms.

Another anomaly in the initial ivermectin experiments was that two outcross strains had much lower EC50 values than the wild-type used, and both strains over-expressed *dyf-3* in the ASE neurons. We performed salt chemotaxis assays to determine if these lower EC50 values were true findings or if the transgene in ASE somehow made the nematode ill (results shown in figure 12). If the transgenes made the worms ill, then we would expect to see abnormal chemotaxis towards NaCl. It appears as if JD702 (over-expresses *dyf-3* and *mCherry* in ASE) has normal chemotaxis behaviour whereas JD698 (over-expresses *dyf-3* and *mCherry* in ASE and AWC) does not. Interestingly, the wild-type worms that do not express the transgene in JD698 also have an abnormal chemotaxis index (CI), indicating that the strain was ill for other reasons. The same situation likely also occurred with JD702, however this strain was re-established because it became ill on NGM plates and frozen worms were not viable. In fact, when JD702 was re-tested with a fresh wild-type strain, their EC50 values were similar ($p<0.012$). It is important to note that the CI is far from 100% for the wild-type strain because the worms probably had too much directional options and by chance chose to move in the salt-absent portion of the plates during the short duration of the assay. To eliminate this error in the future, we could create the salt gradient on one end of a plate and start the worms at the other, instead of in the center, as Luo et. al. have done [57].

Our fourth dye-filling strain, JD687 (rescues ASI and ADE) has one dye-filling sensory neuron with rescued cilia function and appears to be as resistant than *dyf-3(m185)* ($p<0.005$). This indicates one of two things: either one functional dye-filling sensory neuron is not sufficient to

render *C. elegans* sensitive to ivermectin, or the ASI neurons are not important for drug sensitivity. If the latter is true, then the *dyf* gene resistance mechanism may depend on the function of the sensory neurons with specific neuronal connections to make an animal resistant to ivermectin. We also note that rescue of non-dye-filling neurons, such as the IL2 neurons, does not increase ivermectin sensitivity, even though it presumably restores neuronal function. Overall, there is a good correlation between the number of neurons that dye-fill and ivermectin sensitivity. The parsimonious explanation for this correlation is that the *dyf* gene resistance mechanism works by preventing drug entry in the dye-filling sensory neurons.

The most resistant strain was JD687, which rescues *dyf-3* function in ASI and ADE (EC50 ratio of 2.25 versus 1.79 for *dyf-3*-:WT). ASI normally dye-fills and we did see this in the dye-filling assay (see figure 17), however the *daf-7p* did not consistently rescue dye-filling in ASI. There appears to be two sets of sensory neurons that express mCherry in most, if not all worms, however it is clear from the images taken that the shape mCherry takes in one of these pairs of neurons is different from the other mCherry-expressing neurons. If the transgene does rescue ASI successfully, perhaps ASI simply does not play a role in ivermectin resistance. We can test this in the future by injecting the *sra-6p* with *dyf-3*::gpd-3::*mCherry* into SP1603(*m185*) and/or by complementing *dyf-3* under a promoter that expresses only in ASI.

In the theory that neurons with specific modalities must have non-functional cilia to confer ivermectin resistance, nematodes would transmit the anthelmintic to their target GluCl's via the neurons that communicate for muscle contraction. If ivermectin can enter the worm through the sensory neuron cilia, then it can diffuse across the first neuron to an interneuron. From that interneuron, the drug continues down the neuronal network until it reaches the GluCl's. Since ivermectin works as a paralytic to ultimately kill the animal, the sensory neurons necessary for drug resistance would be those whose network terminates in muscles necessary for life (i.e. locomotory and pharyngeal muscles). For example, ASH is one such neuron, with AVA and AVB being some of the intermediate neurons [58]. Another possibility is that the neurons involved in ivermectin resistance are the glutamatergic ones, although this is not likely because ASE is glutamatergic but restoring its cilia does not make *C. elegans* sensitive. We can confirm this by creating more subsets of rescued sensory neurons.

8.2. C. elegans interneuron communication and *dyf-7* ivermectin resistance pathway

The purpose of the following set of experiments was to determine if the *dyf* ivermectin resistance pathway is dependent on any neuronal proteins responsible for interneuron communication. Because sensory neurons with defective cilia are also defective in chemosensation, we wanted to know if lack of sensory input in these neurons caused them to send a signal to activate a stress response. We investigated innexins, which form invertebrate gap junctions that relay signals to downstream cells, the vesicular glutamate transporter protein Eat-4, and the neuropeptide releasing protein Unc-31. Our current data shows that all the proteins examined, with the exceptions of Inx-18 and Inx-19, when non-functional make *C. elegans* hypersensitive to ivermectin ($p<0.01$). This suggests that rather than increasing the vulnerability of the nematode, normal Che-7, Eat-7, Inx-7, and Unc-9 may be necessary for the worm to initiate a stress response to protect itself from ivermectin. If this is true, then we would expect various stress responses to be downregulated or perhaps unresponsive in these strains. This test, however, was not within the scope of this project. We could confirm if the lack of signaling is additive in making the worm ivermectin sensitive by knocking out all these interneuron communication mutants and observe how this strain and its intermediates fair to various doses of ivermectin. This prospective strain and all its intermediate mutants were a goal of this project and are currently in process, however they were not obtained in time to obtain results from ivermectin assays.

The *inx-18(ok2454)* mutant had an EC50 similar to that of the wild-type strain ($p>0.01$), thus it may not play a role in ivermectin resistance. Although individually, the mutant alleles increased ivermectin sensitivity modestly, their effects may be additive. We could test the additivity by creating strains that have subsets of these mutant alleles and observe how the combinations affect *C. elegans* resistance to ivermectin and if any of these strains develop the *dyf* phenotype. It would also be interesting to know if neurotransmission is necessary for ivermectin resistance in dye-filling defective animals. We could test this by making the double mutants on neurotransmission genes and *dyf-3* or *dyf-7*.

One of the mutant alleles observed, with the *inx-19(ky634)* allele, was the only genotype that conferred ivermectin resistance and coincidentally it had the *dyf* phenotype. Thus, the inx-19

mutant strain provided an unanticipated confirmation of the correlation of the *dyf* phenotype and ivermectin resistance. Not much is known about the function of Inx-19, except that it is expressed in 5 of the 6 pairs of dye-filling sensory neurons, among other neurons, and is involved in determining the AWC left-right asymmetric fates [59]. How exactly removing this innexin confers the dye-filling defective phenotype is unclear, although answering this question may provide insight on the *dyf* ivermectin resistance pathway.

8.3. C. elegans stress responses and *dyf-7* ivermectin resistance pathway

In the third part of this project, we aim to determine if the *dyf-3/dyf-7* ivermectin resistance mechanism depends on any stress response pathways. Stress response pathways have been shown to be sensitivity to sensory input providing information about food availability, crowding, osmolarity and temperature. It is reasonable to expect that a change in sensory input caused by the dyf phenotype might trigger a stress response that in turn could affect ivermectin sensitivity. We looked at various transcription factors known to regulate several different pathways including dauer formation, bacterial resistance, oxidative stress (via Daf-16, Skn-1, and Mxl-3), heat shock (via Hsf-1), and other proteins involved in osmotic stress (GPDH-1), oxidative stress (Wrd-23, Gst-4, and Mdt-15). Additionally, we studied the P-glycoproteins (PGP's) because they are known to act as efflux pumps for various nematode toxicants. Thus far we have only completed the ivermectin assay on the *daf-16*, *hsf-1*, *gpdh-1*, and *pgp-1(pk17)::pgp-2(gk114)::pgp-3(pk18)::pgp-9(tm830)::mrp-1(pk89)* mutants. From this preliminary data, we conclude that Daf-16, Hsf-1, and GPDH-1 may play minor roles in saving *C. elegans* from ivermectin intoxication, but that a subset of the PGP's seems necessary for ivermectin resistance in a dye-filling defective mutant.

Similar studies with the PGP mutants have already been done using IVR10, a dye-filling defective strain that may be caused by a frame shift mutation in *dyf*-7 [60]. When Ménez et. al. removed the function of Pgp-1, Pgp-2, Pgp-3, Pgp-9, and Mrp-1, they observed that the ivermectin-selected strain IVR10 upregulates *pgp-1*, *pgp-2*, *pgp-3*, *pgp-9*, and *mrp-1*, among other PGP's. Additionally, when they use a PGP inhibitor, the strain's ivermectin resistance decreases but not to the wild-type EC50 dose [61]. Our results support this research, with our PGP quintuple mutant being almost as sensitive to ivermectin as the wild-type and the quintuple PGP-*dyf-7* double mutant

fairing only marginally better in the anthelmintic. There is a significant difference ($p<0.005$) between each of these strains, indicating that the *dyf-7* resistance pathway is heavily dependent on the subset of PGP's tested here and that they act downstream *dyf-7*. In the sheep parasite *H. contortus*, Pgp-2 and Pgp-9.1 have been shown to interact with ivermectin, suggesting that these two genes in our *C. elegans* PGP mutant subset may be the gene mutations responsible for ivermectin susceptibility [62, 63]. In another experiment, it was shown that loss-of-function of *pgp-2*, *pgp-5*, *pgp-6*, *pgp-7*, *pgp-12*, and *pgp-13* in *C. elegans* resulted in increased ivermectin sensitivity [64]. Again, these experiments support the results seen in this project, that at least one PGP mutant is involved in facilitating ivermectin resistance in both wild-type and *dyf-7* mutant worms.

9. Conclusion

The *dyf* ivermectin resistance pathway is complex but understanding it is relevant to many populations, including countries with endemic human parasites and those with livestock productivity loss issues like ours. Our results are consistent with a mechanism of resistance where naturally-occurring *dyf* phenotype confers ivermectin resistance by preventing the lipophilic drug from entering the sensory neurons of nematodes. We cannot conclude whether interneuron signaling is necessary in the *dyf* resistance pathway in *C. elegans*, although the resistance is dependent on functional efflux pumps as a stress response. There is evidence for the involvement of the PGP's in ivermectin resistance from other papers that support our results.

Our goal in continuing this type of research on ivermectin resistance is to fully understand what makes nematodes resistant and to apply what we learn from *C. elegans* to their parasitic counterparts. Once this is accomplished, we can engineer new drugs that bypass the resistance mechanism, thereby eliminating disease caused by these pests worldwide. Without nematode infestation problems, we will increase the productivity and efficiency in both the livestock industry and any industry that is affected by nematode parasites.

10. References

1. Waghorn TS, Leathwick DM, Rhodes AP, Lawrence KE, Jackson R, Pomroy WE, West DM, Moffat JR: **Prevalence of anthelmintic resistance on sheep farms in New Zealand**. *N Z Vet J* 2006, **54**(6):271-277.
2. Waghorn TS, Leathwick DM, Rhodes AP, Lawrence KE, Jackson R, Pomroy WE, West DM, Moffat JR: **Prevalence of anthelmintic resistance on 62 beef cattle farms in the North Island of New Zealand**. *New Zealand Veterinary Journal* 2006, **54**(6):278-282.
3. Howell SB, Burke, J.M., Miller, J.E., Terrill, T.H., Valencia, E., Williams, M.J., Williamson, L.H., Zajac, A.M., Kaplan, R.M.: **Prevalence of anthelmintic resistance on sheep and goat farms in the southeastern United States**. *Journal of the American Veterinary Medical Association* 2008, **233**(12):1913-1919.
4. Falzon LC, Menzies PI, Shakya KP, Jones-Bitton A, Vanleeuwen J, Avula J, Stewart H, Jansen JT, Taylor MA, Learmount J *et al*: **Anthelmintic resistance in sheep flocks in Ontario, Canada**. *Vet Parasitol* 2013, **193**(1-3):150-162.
5. Walker RS, Miller JE, Monlezun CJ, LaMay D, Navarre C, Ensley D: **Gastrointestinal nematode infection and performance of weaned stocker calves in response to anthelmintic control strategies**. *Vet Parasitol* 2013, **197**(1-2):152-159.
6. Miller CM, Waghorn TS, Leathwick DM, Candy PM, Oliver AM, Watson TG: **The production cost of anthelmintic resistance in lambs**. *Vet Parasitol* 2012, **186**(3-4):376-381.
7. Urdaneta-Marquez L, Bae SH, Janukavicius P, Beech R, Dent J, Prichard R: **A dyf-7 haplotype causes sensory neuron defects and is associated with macrocyclic lactone resistance worldwide in the nematode parasite Haemonchus contortus**. *Int J Parasitol* 2014, **44**(14):1063-1071.
8. Fuse T, Ikeda I, Kita T, Furutani S, Nakajima H, Matsuda K, Ozoe F, Ozoe Y: **Synthesis of photoreactive ivermectin B1a derivatives and their actions on Haemonchus and Bombyx glutamate-gated chloride channels**. *Pestic Biochem Physiol* 2015, **120**:82-90.
9. Cheeseman CL, Delany NS, Woods DJ, Wolstenholme AJ: **High-affinity ivermectin binding to recombinant subunits of the Haemonchus contortus glutamate-gated chloride channel**. *Mol Biochem Parasitol* 2001, **114**(2):161-168.
10. Ward S, Thomson N, White JG, Brenner S: **Electron microscopical reconstruction of the anterior sensory anatomy of the nematode Caenorhabditis elegans.?2UU**. *J Comp Neurol* 1975, **160**(3):313-337.
11. Bargmann CI, Horvitz, H.R.: **Chemosensory Neurons with Overlapping Functions Direct Chemotaxis to Multiple Chemicals in C. elegans.** *Neuron* 1991, **7**:729-742.
12. Suzuki H, Thiele TR, Faumont S, Ezcurra M, Lockery SR, Schafer WR: **Functional asymmetry in Caenorhabditis elegans taste neurons and its computational role in chemotaxis**. *Nature* 2008, **454**(7200):114-117.
13. Bargmann CI, Horvitz HR: **Control of larval development by chemosensory neurons in Caenorhabditis elegans**. *Science* 1991, **251**(4998):1243-1246.
14. Alcedo J, Kenyon C: **Regulation of C. elegans longevity by specific gustatory and olfactory neurons**. *Neuron* 2004, **41**(1):45-55.

15. Sun J, Singh V, Kajino-Sakamoto R, Aballay A: **Neuronal GPCR controls innate immunity by regulating noncanonical unfolded protein response genes**. *Science* 2011, **332**(6030):729-732.
16. Inglis PN: **The sensory cilia of Caenorhabditis elegans**. In., November 27 2006 edn. Wormbook; 2006.
17. Dent JA, Smith MM, Vassilatis DK, Avery L: **The genetics of ivermectin resistance in Caenorhabditis elegans**. *Proc Natl Acad Sci U S A* 2000, **97**(6):2674-2679.
18. Heiman MG, Shaham S: **DEX-1 and DYF-7 establish sensory dendrite length by anchoring dendritic tips during cell migration**. *Cell* 2009, **137**(2):344-355.
19. Murayama T, Toh Y, Ohshima Y, Koga M: **The dyf-3 gene encodes a novel protein required for sensory cilium formation in Caenorhabditis elegans**. *J Mol Biol* 2005, **346**(3):677-687.
20. Inglis PN, Blacque OE, Leroux MR: **Functional Genomics of Intraflagellar Transport-Associated Proteins in C. elegans**. In.; 2009: 267-304.
21. Escher BI, Berger C, Bramaz N, Kwon JH, Richter M, Tsinman O, Avdeef A: **Membrane-water partitioning, membrane permeability, and baseline toxicity of the parasiticides ivermectin, albendazole, and morantel**. *Environ Toxicol Chem* 2008, **27**(4):909-918.
22. Orls M, Sanderson, W.E., Essex, J.W.: **Permeability of Small Molecules through a Lipid Bilayer: A Multiscale Simulation Study**. *Journal of Physical Chemistry B* 2009, **113**:12019–12029.
23. Paula S, Volkov AG, Van Hoek AN, Haines TH, Deamer DW: **Permeation of protons, potassium ions, and small polar molecules through phospholipid bilayers as a function of membrane thickness**. *Biophys J* 1996, **70**(1):339-348.
24. Altun ZF, Chen B, Wang ZW, Hall DH: **High resolution map of Caenorhabditis elegans gap junction proteins**. *Dev Dyn* 2009, **238**(8):1936-1950.
25. White JQ, Jorgensen EM: **Sensation in a single neuron pair represses male behavior in hermaphrodites**. *Neuron* 2012, **75**(4):593-600.
26. Phelan P, Starich TA: **Innexins get into the gap**. *Bioessays* 2001, **23**(5):388-396.
27. Liu P, Chen B, Altun ZF, Gross MJ, Shan A, Schuman B, Hall DH, Wang ZW: **Six innexins contribute to electrical coupling of C. elegans body-wall muscle**. *PLoS One* 2013, **8**(10):e76877.
28. Krzyzanowski MC, Woldemariam S, Wood JF, Chaubey AH, Brueggemann C, Bowitch A, Bethke M, L'Etoile ND, Ferkey DM: **Aversive Behavior in the Nematode C. elegans Is Modulated by cGMP and a Neuronal Gap Junction Network**. *PLoS Genet* 2016, **12**(7):e1006153.
29. Lee RY, Sawin ER, Chalfie M, Horvitz HR, Avery L: **EAT-4, a homolog of a mammalian sodium-dependent inorganic phosphate cotransporter, is necessary for glutamatergic neurotransmission in caenorhabditis elegans**. *J Neurosci* 1999, **19**(1):159-167.
30. Avery L: **The genetics of feeding in Caenorhabditis elegans**. *Genetics* 1993, **133**(4):897-917.
31. Miller KG, Alfonso A, Nguyen M, Crowell JA, Johnson CD, Rand JB: **A genetic selection for Caenorhabditis elegans synaptic transmission mutants**. *Proc Natl Acad Sci U S A* 1996, **93**(22):12593-12598.

32. Ann K, Kowalchyk JA, Loyet KM, Martin TF: **Novel Ca2+-binding protein (CAPS) related to UNC-31 required for Ca2+-activated exocytosis**. *J Biol Chem* 1997, **272**(32):19637-19640.
33. Xu C, Li CY, Kong AN: **Induction of phase I, II and III drug metabolism/transport by xenobiotics**. *Arch Pharm Res* 2005, **28**(3):249-268.
34. Blackwell TK, Steinbaugh MJ, Hourihan JM, Ewald CY, Isik M: **SKN-1/Nrf, stress responses, and aging in Caenorhabditis elegans**. *Free Radic Biol Med* 2015, **88**(Pt B):290-301.
35. Oliveira RP, Porter Abate J, Dilks K, Landis J, Ashraf J, Murphy CT, Blackwell TK: **Condition-adapted stress and longevity gene regulation by Caenorhabditis elegans SKN-1/Nrf**. *Aging Cell* 2009, **8**(5):524-541.
36. Tullet JM, Hertweck M, An JH, Baker J, Hwang JY, Liu S, Oliveira RP, Baumeister R, Blackwell TK: **Direct inhibition of the longevity-promoting factor SKN-1 by insulin-like signaling in C. elegans**. *Cell* 2008, **132**(6):1025-1038.
37. Lee D, Son HG, Jung Y, Lee SV: **The role of dietary carbohydrates in organismal aging**. *Cell Mol Life Sci* 2017, **74**(10):1793-1803.
38. Garsin DA, Villanueva JM, Begun J, Kim DH, Sifri CD, Calderwood SB, Ruvkun G, Ausubel FM: **Long-lived C. elegans daf-2 mutants are resistant to bacterial pathogens**. *Science* 2003, **300**(5627):1921.
39. Nelson DW, Padgett RW: **Insulin worms its way into the spotlight**. *Genes Dev* 2003, **17**(7):813-818.
40. Lamitina T, Huang CG, Strange K: **Genome-wide RNAi screening identifies protein damage as a regulator of osmoprotective gene expression**. *Proc Natl Acad Sci U S A* 2006, **103**(32):12173-12178.
41. Lamitina ST, Strange K: **Transcriptional targets of DAF-16 insulin signaling pathway protect C. elegans from extreme hypertonic stress**. *Am J Physiol Cell Physiol* 2005, **288**(2):C467-474.
42. Choe KP, Przybysz AJ, Strange K: **The WD40 repeat protein WDR-23 functions with the CUL4/DDB1 ubiquitin ligase to regulate nuclear abundance and activity of SKN-1 in Caenorhabditis elegans**. *Mol Cell Biol* 2009, **29**(10):2704-2715.
43. Goh GY, Martelli KL, Parhar KS, Kwong AW, Wong MA, Mah A, Hou NS, Taubert S: **The conserved Mediator subunit MDT-15 is required for oxidative stress responses in Caenorhabditis elegans**. *Aging Cell* 2014, **13**(1):70-79.
44. Grove CA, De Masi F, Barrasa MI, Newburger DE, Alkema MJ, Bulyk ML, Walhout AJ: **A multiparameter network reveals extensive divergence between C. elegans bHLH transcription factors**. *Cell* 2009, **138**(2):314-327.
45. Taubert S, Van Gilst MR, Hansen M, Yamamoto KR: **A Mediator subunit, MDT-15, integrates regulation of fatty acid metabolism by NHR-49-dependent and -independent pathways in C. elegans**. *Genes Dev* 2006, **20**(9):1137-1149.
46. Paek J, Lo JY, Narasimhan SD, Nguyen TN, Glover-Cutter K, Robida-Stubbs S, Suzuki T, Yamamoto M, Blackwell TK, Curran SP: **Mitochondrial SKN-1/Nrf mediates a conserved starvation response**. *Cell Metab* 2012, **16**(4):526-537.
47. Tawe WN, Eschbach ML, Walter RD, Henkle-Duhrsen K: **Identification of stress-responsive genes in Caenorhabditis elegans using RT-PCR differential display**. *Nucleic Acids Res* 1998, **26**(7):1621-1627.

48. Kubagawa HM, Watts JL, Corrigan C, Edmonds JW, Sztul E, Browse J, Miller MA: **Oocyte signals derived from polyunsaturated fatty acids control sperm recruitment in vivo**. *Nat Cell Biol* 2006, **8**(10):1143-1148.
49. Sheps JA, Ralph S, Zhao Z, Baillie DL, Ling V: **The ABC transporter gene family of Caenorhabditis elegans has implications for the evolutionary dynamics of multidrug resistance in eukaryotes**. *Genome Biol* 2004, **5**(3):R15.
50. Broeks A, Janssen HW, Calafat J, Plasterk RH: **A P-glycoprotein protects Caenorhabditis elegans against natural toxins**. *EMBO J* 1995, **14**(9):1858-1866.
51. Broeks A, Gerrard B, Allikmets R, Dean M, Plasterk RH: **Homologues of the human multidrug resistance genes MRP and MDR contribute to heavy metal resistance in the soil nematode Caenorhabditis elegans**. *EMBO J* 1996, **15**(22):6132-6143.
52. Mahajan-Miklos S, Tan MW, Rahme LG, Ausubel FM: **Molecular mechanisms of bacterial virulence elucidated using a Pseudomonas aeruginosa-Caenorhabditis elegans pathogenesis model**. *Cell* 1999, **96**(1):47-56.
53. Mello CC, Kramer JM, Stinchcomb D, Ambros V: **Efficient gene transfer in C.elegans: extrachromosomal maintenance and integration of transforming sequences**. *EMBO J* 1991, **10**(12):3959-3970.
54. Li H, Avery L, Denk W, Hess GP: **Identification of chemical synapses in the pharynx of Caenorhabditis elegans**. *Proc Natl Acad Sci U S A* 1997, **94**(11):5912-5916.
55. Huang XY, Hirsh D: **A second trans-spliced RNA leader sequence in the nematode Caenorhabditis elegans**. *Proc Natl Acad Sci U S A* 1989, **86**(22):8640-8644.
56. Chou JH, Bargmann CI, Sengupta P: **The Caenorhabditis elegans odr-2 gene encodes a novel Ly-6-related protein required for olfaction**. *Genetics* 2001, **157**(1):211-224.
57. Luo L, Wen Q, Ren J, Hendricks M, Gershow M, Qin Y, Greenwood J, Soucy ER, Klein M, Smith-Parker HK *et al*: **Dynamic encoding of perception, memory, and movement in a C. elegans chemotaxis circuit**. *Neuron* 2014, **82**(5):1115-1128.
58. Zheng Y, Brockie PJ, Mellem JE, Madsen DM, Maricq AV: **Neuronal control of locomotion in C. elegans is modified by a dominant mutation in the GLR-1 ionotropic glutamate receptor**. *Neuron* 1999, **24**(2):347-361.
59. Chuang CF, Vanhoven MK, Fetter RD, Verselis VK, Bargmann CI: **An innexin-dependent cell network establishes left-right neuronal asymmetry in C. elegans**. *Cell* 2007, **129**(4):787-799.
60. Janukavicius P: **dyf-7 is responsible for the low-levels of ivermectin resistance in Caenorhabditis elegans strains IVR6 and IVR10**. Montreal: McGill University; 2012.
61. Menez C, Alberich M, Kansoh D, Blanchard A, Lespine A: **Acquired Tolerance to Ivermectin and Moxidectin after Drug Selection Pressure in the Nematode Caenorhabditis elegans**. *Antimicrob Agents Chemother* 2016, **60**(8):4809-4819.
62. Godoy P, Lian J, Beech RN, Prichard RK: **Haemonchus contortus P-glycoprotein-2: in situ localisation and characterisation of macrocyclic lactone transport**. *Int J Parasitol* 2015, **45**(1):85-93.
63. Godoy P, Che H, Beech RN, Prichard RK: **Characterisation of P-glycoprotein-9.1 in Haemonchus contortus**. *Parasit Vectors* 2016, **9**:52.
64. Ardelli BF, Prichard RK: **Inhibition of P-glycoprotein enhances sensitivity of Caenorhabditis elegans to ivermectin**. *Vet Parasitol* 2013, **191**(3-4):264-275.

11. Appendix

11.1. Complemented *dyf-3* strains: mCherry expression and dye-filling

Appendix Figure 16. Images taken of the *dyf-3*-complemented strain under *ceh-36* in a *dyf-3* knockout background (strain JD688, left top and bottom) and in a wild-type background (strain JD698, right top and bottom). The top images show the fluorescence of expressed mCherry and the bottom images show the fluorescence of sensory neurons that dye-fill with DiO. *Ceh-36p* is expected to express *dyf-3* and *mCherry* in the ASE sensory neurons.

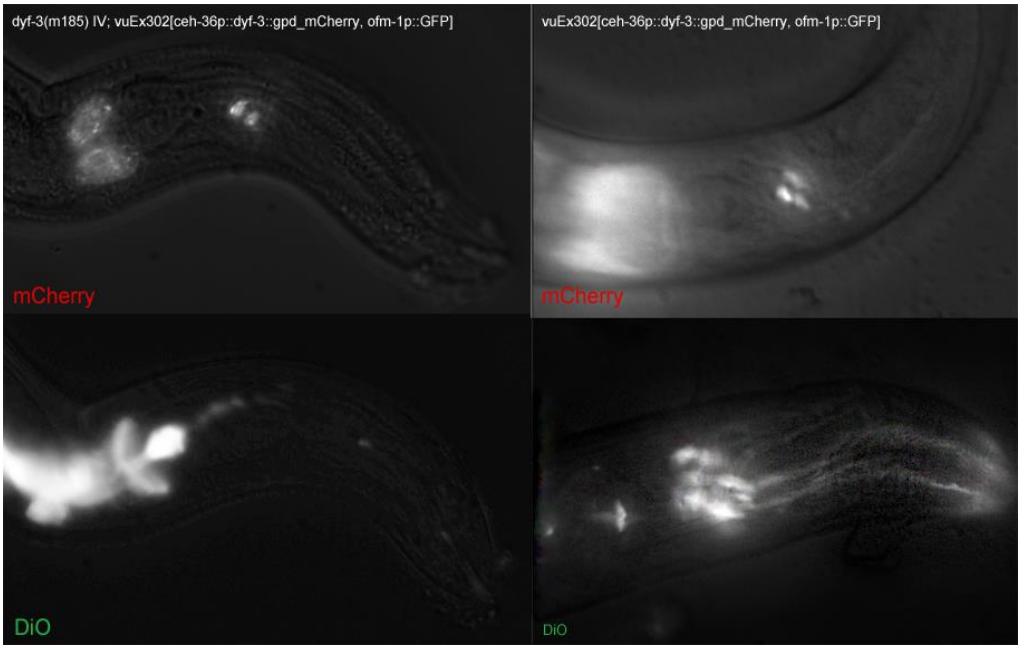

Appendix Figure 17. Images taken of the *dyf-3*-complemented strain under *daf-7p* in a *dyf-3* knockout background (strain JD687, left top and bottom) and in a wild-type background (strain JD697, right top and bottom). The top images show the fluorescence of expressed mCherry and the bottom images show the fluorescence of sensory neurons that dye-fill with DiO. *Daf-7p* is expected to express *dyf-3* and *mCherry* in the ASI and ADE sensory neurons.

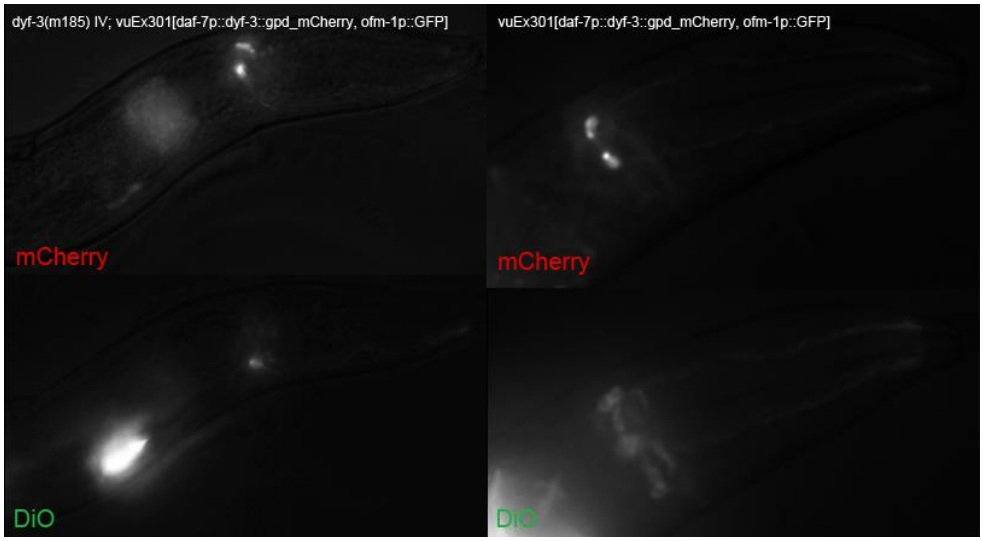

Appendix Figure 18. Images taken of the *dyf-3*-complemented strain under *gcy-5p* and *gcy-7p* in a *dyf-3* knockout background (strain JD692, left top and bottom) and in a wild-type background (strain JD702, right top and bottom). The top images show the fluorescence of expressed mCherry and the bottom images show the fluorescence of sensory neurons that dye-fill with DiO. *Gcy-5p* and *Gcy-7p* are expected to express *dyf-3* and *mCherry* in the ASE(R) and ASE(L) sensory neurons respectively.

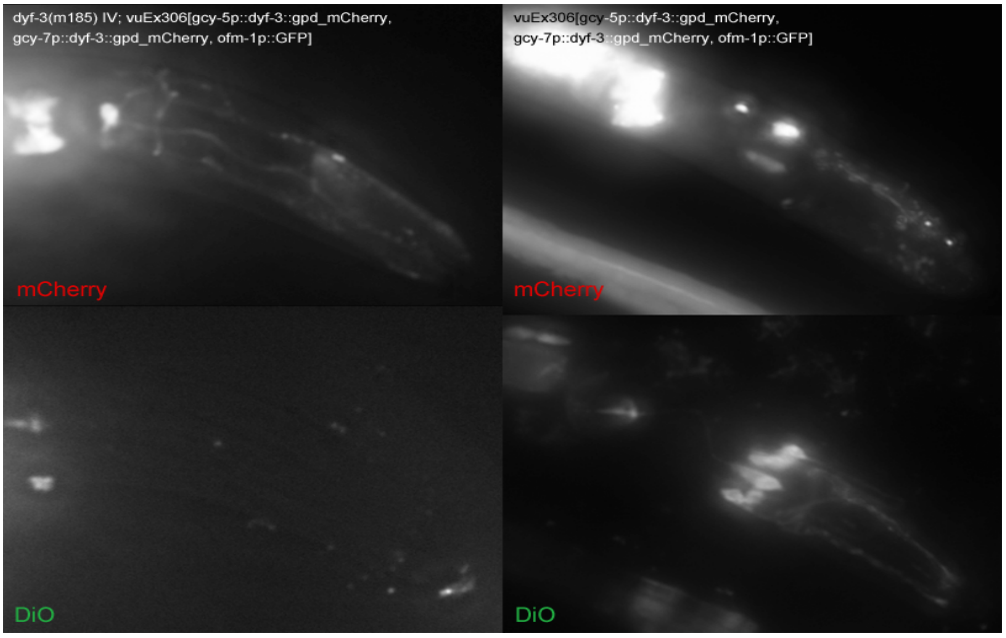

Appendix Figure 19. Images taken of the *dyf-3*-complemented strain under *klp-6p* in a *dyf-3* knockout background (strain JD686, left top and bottom) and in a wild-type background (strain JD696, right top and bottom). The top images show the fluorescence of expressed mCherry and the bottom images show the fluorescence of sensory neurons that dye-fill with DiO. *Klp-6* is expected to express *dyf-3* and *mCherry* in the IL2 sensory neurons.

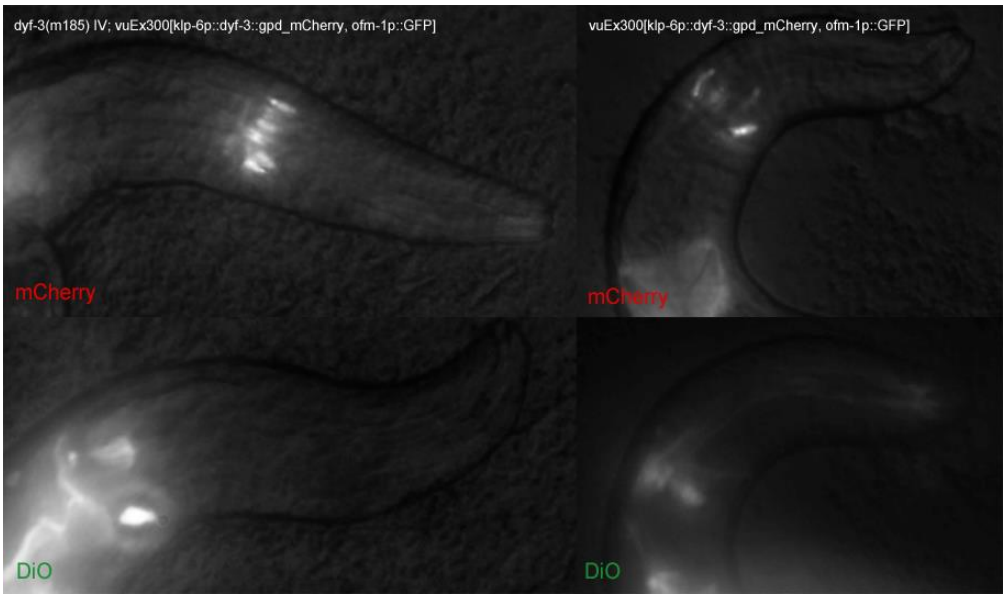

Appendix Figure 20. Images taken of the *dyf-3*-complemented strain under *odr-2p* in a *dyf-3* knockout background (strain 691, left top and bottom) and in a wild-type background (strain JD701, right top and bottom). The top images show the fluorescence of expressed mCherry and the bottom images show the fluorescence of sensory neurons that dye-fill with DiO. *Odr-2p* is expected to express *dyf-3* and *mCherry* in the IL2 and ASG sensory neurons as well as several interneurons.

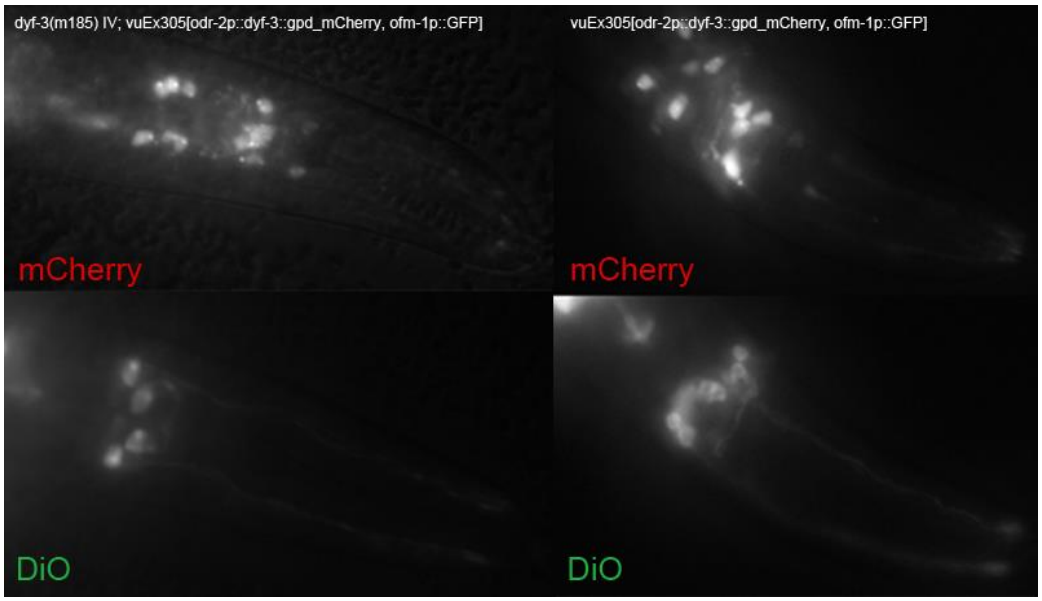

Appendix Figure 21. Images taken of the *dyf-3*-complemented strain under *sre-1p* in a *dyf-3* knockout background (strain 685, left) and in a wild-type background (strain JD695, right). The images show the fluorescence of sensory neurons that dye-fill with DiO. *Sre-1p* is expected to express *dyf-3* in the ADL and ASJ sensory neurons.

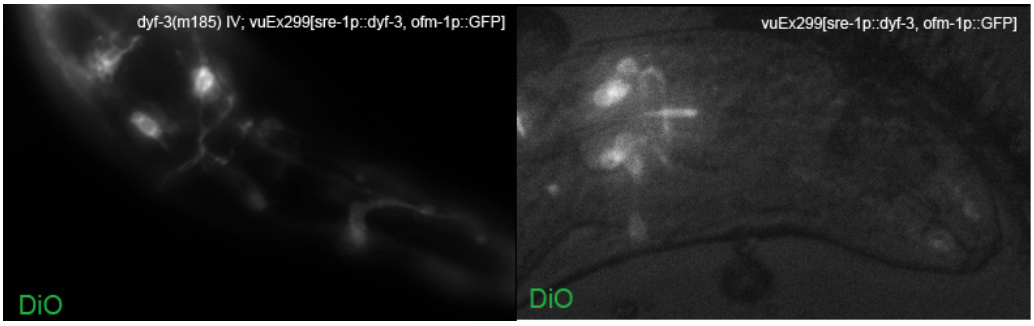

Appendix Figure 22. Images taken of the *dyf-3*-complemented strain under *srh-11p* in a *dyf-3* knockout background (strain JD690, left top and bottom) and in a wild-type background (strain JD700, right top and bottom). The top images show the fluorescence of expressed mCherry and the bottom images show the fluorescence of sensory neurons that dye-fill with DiO. *Srh-11p* is expected to express *dyf-3* and *mCherry* in the ASJ sensory neurons.

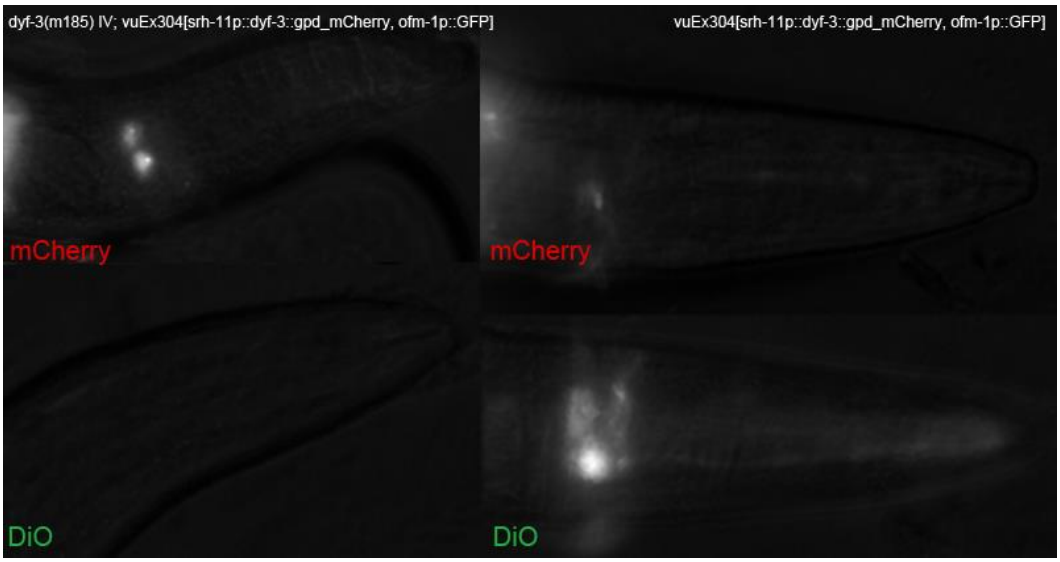

Appendix Figure 23. Images taken of the *dyf-3*-complemented strain under *srh-142p* in a *dyf-3* knockout background (strain JD689, left top and bottom) and in a wild-type background (strain JD699, right top and bottom). The top images show the fluorescence of expressed mCherry and the bottom images show the fluorescence of sensory neurons that dye-fill with DiO. *Srh-142p* is expected to express *dyf-3* and *mCherry* in the ADF sensory neurons.

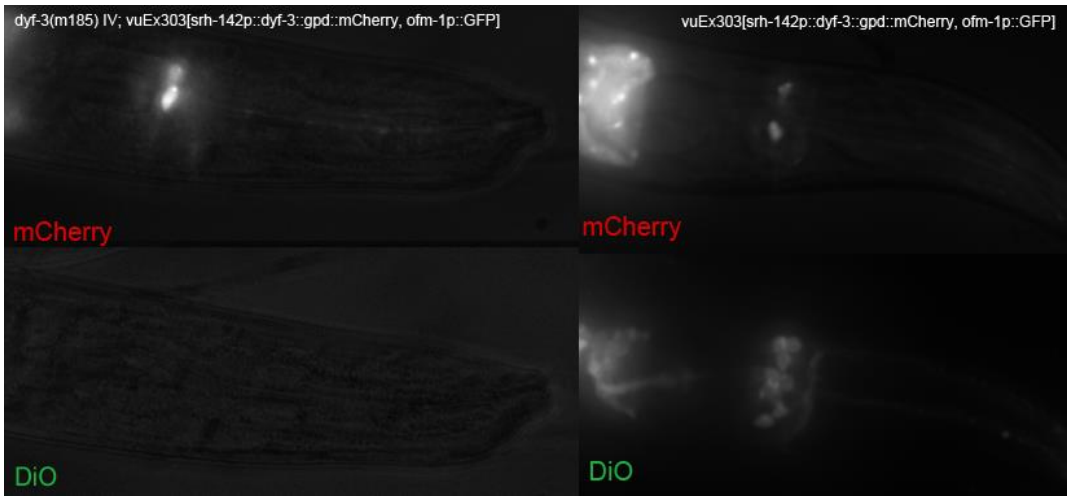

Appendix Figure 24. Images taken of the *dyf-3*-complemented strain under *sre-1p* and *sra-6p* in a *dyf-3* knockout background (strain JD663, left) and in a wild-type background (strain JD704, right). The images show the fluorescence of sensory neurons that dye-fill with DiO. *Sre-1p* is expected to express *dyf-3* in the ADL and ASJ sensory neurons and *sra-6p* is expected to express *dyf-3* in the ASH and ASI sensory neurons.

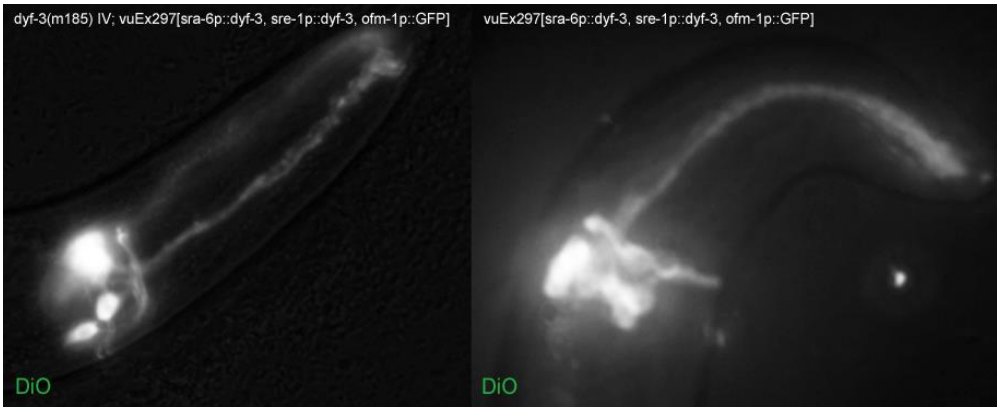

11.2. EPG readings

Figure 25. Shows the EPG current reading from the N2 strain JD29. The E phase (muscle cell depolarization) is followed by inhibitory postsynaptic potentials, then by the R phase (repolarization, muscle relaxation).

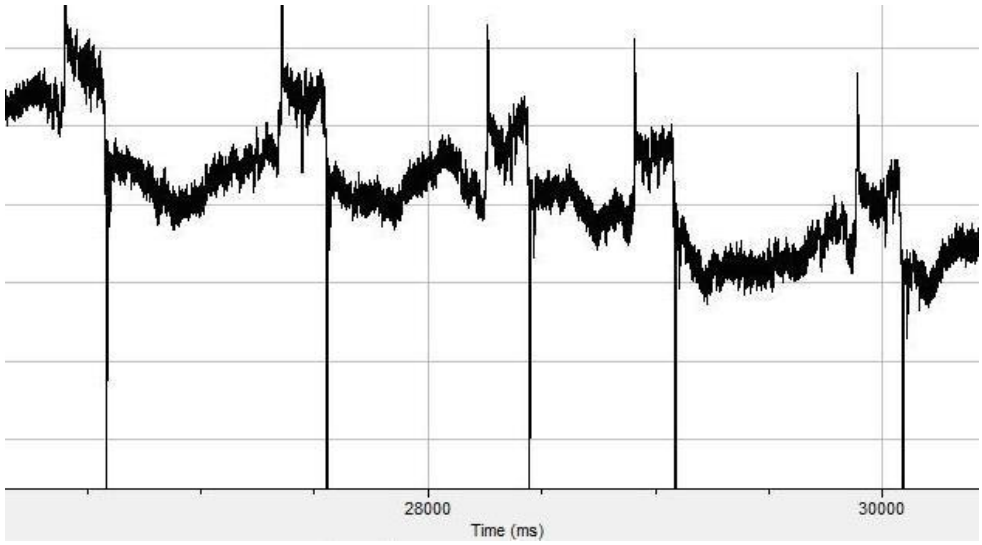

Figure 26. Shows the EPG reading from RB1896, the *inx-18(ok2454)* strain. This strain appears to have a normal E phase and R phase, however the P phase (plateau) in between the two appears to have more variability in the current.

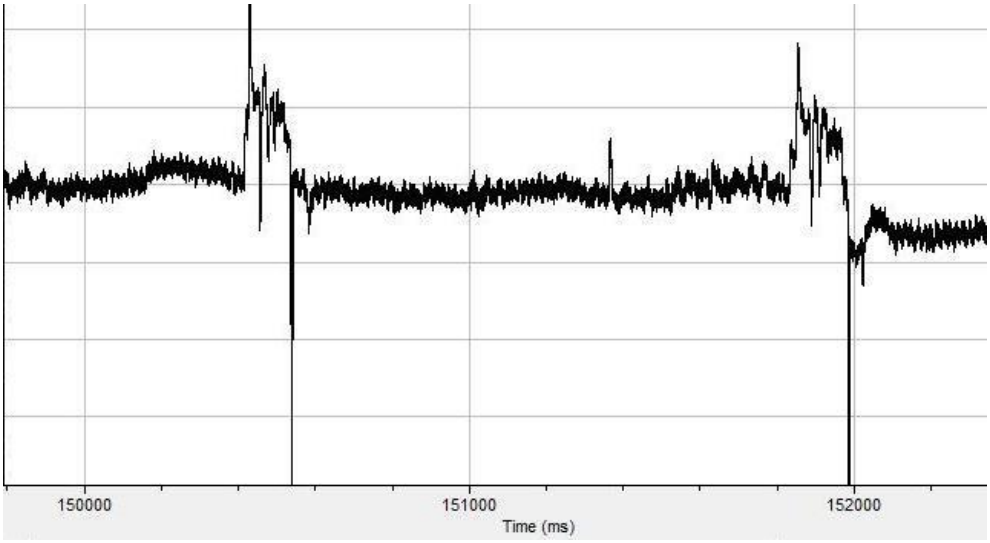

Figure 27. Shows the EPG current reading from MT6304, the *eat-4(ky5)* mutant. These mutants have a weak E phase with a prolonged P phase [54].